Matrix metalloproteinases as promising regulators of axonal regrowth in the injured adult zebrafish retinotectal system

SCHOLARONE™
Manuscripts

Matrix metalloproteinases as promising regulators of axonal regrowth in the injured adult zebrafish retinotectal system

Kim Lemmens[1], Ilse Bollaerts[1], Stitipragyan Bhumika[2], Lies De Groef[1], Jessie Van houcke[1], Veerle M. Darras[2], Inge Van Hove[1], Lieve Moons[1*]

[1]Laboratory of Neural Circuit Development and Regeneration, Biology Department, KU Leuven, B-3000 Leuven, Belgium

[2]Laboratory of Comparative Endocrinology, Biology Department, KU Leuven, B-3000 Leuven, Belgium

Abbreviated Title: MMP roles in the regenerative zebrafish retina

Associate Editor: Thomas E. Finger

Key words: optic nerve crush, regeneration, MMP inhibitor studies, spatiotemporal expression pattern, retina, AB_1657437, AB_1565437, AB_2144746, AB_881233, AB_627659, AB_477593, AB_477171, AB_2069697, AB_528480

*Corresponding author: Dr. Lieve Moons**,** Research Group Neural Circuit Development and Regeneration, Department of Biology, Naamsestraat 61, box 2464**,** B-3000 Leuven, BELGIUM, Phone: +32-16-323991**,** Fax: +32-16-324262

lieve.moons@bio.kuleuven.be

Abstract

Overcoming the failure of axon regeneration in the mammalian central nervous system (CNS) after injury remains a major challenge, which makes the search for regenerative molecules essential. Matrix metalloproteinases (MMPs) have sporadically been shown to affect axonal outgrowth during CNS development and to increase their expression during CNS repair. However, *in vivo* evidence for a contribution of MMPs in axonal regrowth seems limited. We therefore investigated the role of MMPs in optic nerve regeneration following optic nerve crush (ONC) in adult zebrafish, which spontaneously and fully recover from such injuries. We show that lowering general retinal MMP activity through intravitreal injections of GM6001 after ONC strongly reduces retinal ganglion cell (RGC) axonal regrowth without influencing RGC survival. Based on a recently performed transcriptome profiling study, we subsequently followed the expression pattern of four MMPs after ONC via combined use of Western blotting and immunostainings. Mmp-2 and -13a were found increasingly present in RGC somata during axonal regrowth. Moreover, Mmp-2 and -9 became respectively upregulated in regrowing RGC axons and inner plexiform layer (IPL) synapses. In contrast, after an initial rise in IPL neurites and RGC axons during the injury response, Mmp-14 expression decreased during regeneration. Altogether, a phase dependent expression pattern for each specific MMP was observed, implying them in axonal regrowth and inner retina remodeling. In conclusion, our data indicate that retinally expressed MMPs are involved in RGC axonal regrowth, which could favor these enzymes or their downstream targets as potential regenerative molecules for the injured mammalian CNS.

Introduction

Optic neuropathies, characterized by progressive retinal ganglion cell (RGC) axonal degeneration and death, are becoming more and more prevalent in our elderly population. As adult mammals lack the robust capacity to replace or repair damaged axons, i.e. axonal regeneration, or injured neurons, optic nerve damage often results in irreversible blindness (Horner and Gage, 2000; Benowitz and Yin, 2007; Huebner and Strittmatter, 2009). Up to now, considerable progress has been made by studying both, intrinsic and experimentally induced, optic nerve regeneration in adult mammals. As such, it has been demonstrated that a partial axonal regeneration with minor visual functional recovery can be obtained, not only through modifications of the suppressive extracellular matrix (ECM) and the administration of trophic support molecules, but also via the induction of restricted ocular inflammation and glial reactivity (Berry et al., 2008; Kurimoto et al., 2010; Benowitz and Popovich, 2011; de Lima et al., 2012; Lorber et al., 2012; Kurimoto et al., 2013). However, a complete restoration of mammalian vision has not yet been achieved.

In contrast to mammals, adult zebrafish can fully functionally recover from an optic nerve injury, as a substantial part of the damaged RGCs possesses the ability to survive, regrow long-distance axons and re-establish synaptic contacts with their target neurons, all within 3 weeks post-injury (Becker and Becker, 2008; Kaneda et al., 2008; McCurley and Callard, 2010; Wyatt et al., 2010; Cerveny et al., 2012; Zou et al., 2013). This flawless axonal regeneration of RGCs towards the optic tectum (OT), i.e. retinotecal regeneration, is likely due to an increased expression of growth- and pathfinding-associated genes in regenerating RGCs and an environment containing less inhibitory, but more axonal regrowth promoting molecules in comparison to the mammalian visual system (Becker and Becker, 2007a; b). Nevertheless, an increasing number of studies report a remarkable similarity in the signaling pathways underlying central nervous system (CNS) regeneration in zebrafish and mammals. Therefore, these teleost fish are suggested as a suitable model organism for the identification of regeneration enhancing molecules for the injured mammalian CNS (Fleisch et al., 2011; Wang and Jin, 2011; Becker and Becker, 2014; Elsaeidi et al., 2014).

Matrix metalloproteinases (MMPs) are members of the metzincin superfamily named after the zinc ion and the conserved Methionine residue at the active site (Nagase et al., 2006). These proteinases are predominantly known for their ability to cleave and remodel the ECM, although they also (in)activate many signaling molecules such as growth factors, adhesion molecules and cytokines (Page-McCaw et al., 2007; Morrison et al., 2009) and are nowadays

even reported to function intracellularly (Cauwe and Opdenakker, 2010). Besides playing an important role in the developing and healthy adult CNS (Agrawal et al., 2008), MMPs have repeatedly been associated with the onset of neurodegenerative diseases and CNS injuries (Sternlicht and Werb, 2001; Yong et al., 2007). Nonetheless, it is becoming increasingly clear that MMPs, and especially the gelatinases, MMP-2 and -9, could be benefactors in the repair and regeneration of the adult mammalian CNS (Verslegers et al., 2013a). Remarkably, a vast amount of studies implies MMPs as key players in the degradation of inhibitory molecules around the injury site, thereby clearing the path for axons to regrow. For example, in adult rats, triggered to regenerate axons across the injury site of damaged spinal cords and optic nerves, gelatinase activity was strongly induced in the scar tissue, thus seemingly necessary to degrade the inhibitory environment (Duchossoy et al., 2001a; Duchossoy et al., 2001b; Ahmed et al., 2005). Indeed, several independent studies identified MMP-2 as a major proteinase able to reduce the glial scar through cleavage of chondroitin sulfate proteoglycans (CSPGs) (Hsu et al., 2006; Pastrana et al., 2006; Veeravalli et al., 2009; Filous et al., 2010). Notably, also MMP-3, -7 and -8 seem able to overcome CSPG inhibition in cultured primary mouse cortical neurons, resulting in an enhanced neurite outgrowth (Cua et al., 2013).

Also in lower vertebrates, MMPs have been cited as potential regenerative targets. In axolotls, MMP-1, -2 and -9 were shown to be upregulated during spinal cord regeneration, while their expression declined as regeneration was nearly completed (Chernoff, 1996; Chernoff et al., 2000). Furthermore, RT-PCR and microarray studies performed on the regenerating zebrafish eye at different time points after optic nerve crush (ONC), show a stringent correlation between MMP expression and CNS regeneration (McCurley and Callard, 2010). Indeed, four different MMPs (*mmp-2, -9, -13a* and *-14*) were found to be upregulated during distinct phases of retinotectal regeneration. In detail, *mmp-9* and *-13a* were classified within the top ten upregulated genes during the injury response phase. Yet, while the expression of *mmp-9*, together with *mmp-2* and *-14*, augmented during the axonal outgrowth phase, *mmp-13a* mRNA levels were shown to gradually decline. Also in this model, MMP expression decreased near completion of regeneration (McCurley and Callard, 2010). As zebrafish are stated to have a strongly reduced inhibitory environment, a thorough study of MMP functioning in zebrafish retinotectal regeneration, could potentially unravel new MMP driven regenerative processes, apart from mammalian glial scar breakdown. Therefore, within this study we aimed at shedding light on the importance of MMPs in zebrafish optic nerve regeneration by interfering with their activity *in vivo* and by determining their spatiotemporal expression pattern after ONC.

Material and methods

Zebrafish maintenance

Zebrafish (*Danio rerio*) were maintained under standard laboratory conditions at 28°C on a 14 h light/10 h dark cycle. Fish were fed twice daily with a combination of dry food and brine shrimp. All experiments were performed on equal-sized adult zebrafish (AB wild-type) of 5 months old. All animal experiments were approved by the KU Leuven Animal Ethics Committee and executed in strict accordance with the European Communities Council Directive of 20 October 2010 (2010/63/EU).

Optic nerve crush (ONC)

Optic nerve (ON) injury was performed as previously described (Becker et al., 2000; Zou et al., 2013). Briefly, zebrafish were anesthetized in a 0.03% solution of tricaine (MS-222, Sigma Aldrich) and put under a dissecting microscope (Leica) on a moist tissue paper, left side facing upward. The connective tissue surrounding the left eye was removed with a pair of sterile forceps (Dumont No. 5, FST). Subsequently, the eyeball was lifted out of its orbit, thereby exposing the optic nerve and ophthalmic artery. Sterile forceps were carefully placed around the left ON, which was crushed for 10 s at 1 mm distance of the ON head, thereby avoiding damage to the ophthalmic artery. A successful ONC was indicated by a clear stripe across the whitish ON at the site where the forceps had been applied. After surgery, fish were returned to separate tanks to recover. External/independent sham-operated and unharmed, naive eyes were used as control for spatiotemporal expression studies, in agreement with recent publications reporting contralateral effects of eye/optic nerve injuries (Gallego et al., 2012; Neve et al., 2012). The operation procedure for the sham group included all steps above, except the actual crushing of the ON.

Histology, immunohistochemistry and histomorphometric analysis

For all histological and immunohistochemical (IHC) stainings, fish were euthanized by submersion in 0.1% tricaine. Adult eyes of fish at various stages post-injury (0, 6 hours and 1, 4, 7, 10, 14, 18, 21 days post-injury (h/dpi) were dissected and fixed overnight in 4% paraformaldehyde (PFA) in phosphate buffered saline (PBS) and processed for cryosectioning (10 μm sections). General retinal morphology was studied by H&E staining. Immunostainings were performed by using the following primary antibodies: rabbit anti-MMP-2 (Santa Cruz

Biotechnology, sc-8835-R), rabbit anti-Mmp-9 (Anaspec, AS-55345), rabbit anti-Mmp-13a (Anaspec, AS-55114) and rabbit anti-MMP-14 (Abcam, ab53712), and subsequently detected with a horseradish peroxidase (HRP)-labeled goat-anti-rabbit antibody (Dako), using the TSA™ FT/Cy3 System (PerkinElmer). For an adequate determination of retinal MMP localization, sections from minimally 3 fish per post-injury stage were stained. Additional stainings were performed on similar sections, using Alexa Fluor secondary antibodies (Invitrogen) or the TSA™ FT/Cy3 amplification system for the following primary antibodies: mouse anti-GAP-43 (Santa Cruz Biotechnology, sc-33705) mouse anti-α-tubulin (Sigma Aldrich, T9026), mouse anti-MAP2 (2a + 2b) (Sigma Aldrich, M1406), rabbit anti-activated Caspase-3 (Biovision, 3015-100) and mouse anti-SV2 (Developmental Studies Hybridoma Bank). Fluorescent imaging was performed using an Olympus FV1000 confocal microscope at 20x or 60x magnification. Histological pictures were acquired with a microscope Zeiss imager Z1 at 20x magnification. For morphometric analysis of retinal thickness, measurements were made on 6 retinal sections per fish, immediately adjacent to the optic nerve from at minimum 5 fish per condition, using Image J software. Lastly, to check for differences in apoptosis, the percentage of apoptotic cells in the entire RGC layer was calculated by determining the ratio of activated Caspase-3$^+$ cells/DAPI$^+$ cells on 6 retinal sections immediately adjacent to the optic nerve from at least 5 retinas per condition. Besides, on the same retinal sections the number of DAPI$^+$ cells per 100μm RGC layer was counted, serving as an additional confirmative analysis method to visualize possible neurodegeneration.

Western blotting (WB)

Fish were sacrificed (0,1% tricaine), retinas were dissected at 0, 6 hpi and at 1, 4, 7, 10, 14, 18 and 21 dpi after ONC or sham operation, and homogenized in lysis buffer (10 mM Tris-HCl pH 8, 1% Triton X-100, 150 mM NaCl, 0.1% SDS, 0.5% sodium deoxycholate, 0.2% sodium azide), supplemented with protease inhibitors (Roche). Each sample contained a pool of 5 retinas. Protein concentrations were determined via the Bradford method. Homogenates were loaded at 10 μg on a 4-12% SDS-PAGE and depending on the primary antibody transferred onto a Polyvinylidine Fluoride (PVDF) (MMP-2, -9, -13a, GAP-43) or nitrocellulose (MMP-14) membrane. Membranes were incubated for 2 h in 5% Amersham ECL Blocking Agent (GE Healtcare, RPN2125) in Tris buffered saline (TBS) and put overnight with the following primary antibodies: rabbit anti-MMP-2 (Santa-Cruz Biotechnology, sc-8835-R), rabbit anti-Mmp-9 (Anaspec, AS-55345), rabbit anti-Mmp-13a

(Anaspec, AS-55114), rabbit anti-MMP-14 (Abcam, ab53712), mouse anti-GAP-43 (Santa Cruz Biotechnology, sc-33705). The next day, a 45' incubation with the appropriate HRP-labeled secondary antibodies (Dako, 1:5000–1:100000) was performed. Protein bands were visualized using a luminol-based enhanced chemiluminescent kit (Thermo Scientific) by means of an imaging system (Biorad, ChemiDoc MP imaging system). Protein bands were semi-quantitatively evaluated by densitometry (Image Lab 4.1, Biorad). Coomassie blue staining of the membranes was used as a loading control and optical density values of protein bands were normalized to corresponding bands of the total protein stain to correct for interlane variability of protein loading (Li and Shen, 2013). Values from ONC samples were plotted as a relative percentage to the values of sham-operated retinal homogenates of the same time point after surgery, which was put at 100%. Each experiment was performed 3 times, using minimally 3 different pools of retinal samples per condition.

Antibody characterization

All antibodies used in the present study are summarized in Table 1. The rabbit polyclonal antibodies anti-MMP-2 and anti-MMP-14 were both raised to a synthetic peptide corresponding to the C-terminus of human MMP-2 and MMP-14 respectively. In detail, rabbit anti-MMP-2 was raised to a human synthetic peptide mapping within the region of amino acids 600-650: PGFPKLIADAWNAIPDNLDAVVDLQGGGHSYFFKGAYYLKLENQSLK SVKF. Rabbit anti-MMP-14 was developed to human synthetic peptide amino acid sequence: DEVFTYFYKGNKYWKFNNQKLKVEPGYPKSALRDWMGCPSGGRPDEGTEE (aa 471-520). The used MMP-2 and MMP-14 antibodies respectively have the ZFIN antibody identifiers ZDB-ATB-130220-4 and ZDB-ATB-130220-2. These antibodies have been extensively characterized and evaluated for their specificity in the zebrafish visual system by our research group through WB and IHC in a study by Janssens et al. (2013). Here, we revalidated those antibodies by using embryonic zebrafish lysates as positive controls (Fig. 5) and found them to label bands at the expected molecular masses (Mmp-2: pro form: 72 kDa, active form: 64 kDa; mature Mmp-14: 55-60 kDa). Moreover, we report a similar localization of Mmp-2 and -14 on adult zebrafish retinal sections as compared to the developing zebrafish and mammalian visual system. Both, rabbit polyclonal antibodies to Mmp-9 and Mmp-13a were raised against the hinge region of their respective zebrafish MMPs (NP_998288 and NP_958911) to guarantee species reactivity to zebrafish. The peptide sequence used to produce the anti-Mmp-9 antibody locates in the region of amino acids 440-480: QYLYGPRTGPEPTAPQPRTTTSSPVVPTKPSPSDKTTTAST. For the anti-Mmp-13a

antibody, the immunogen sequence was designed within the region of amino acids 185-285: LAHAYPPYEGVGGDAHFDDDETFSYRSPQYYTLFSVAAHEFGHSLGLGHSRDPGAL MYPTYVYRDMDRFILPRDDVNGIQSLYGPNTDVNTDDSKPTPPVT. Both antibodies have been validated profoundly by the manufacturer, Anaspec, who confirmed antibody reactivity by ELISA. The specificity was equally assured through western blot analysis of zebrafish lysate and by blocking the antibodies with proper immunizing peptides (see manufacturers datasheet). Also we detected identical molecular masses for both MMPs (Mmp-9: pro form: 92 kDa, active form: 76 kDa; Mmp-13a: pro form: 80 kDa, active form: 45 kDa) in lysates of adult zebrafish eyes and/or appropriate controls, thereby confirming the manufacturers observations. Moreover, experimental data obtained with the Mmp-13a antibody have been published before (Petrey et al., 2012). Mouse anti-GAP-43 has been raised against the full length GAP-43 of rat origin. This antibody produced a staining pattern similar to previous reports in the adult mouse and zebrafish retina (Kapfhammer et al., 1997; Diekmann et al., 2015) and detects a 20-25 kDa band on WB analysis of adult zebrafish eyes lysate as predicted by several online peptide mass calculators (Q6DG93-1). Rabbit anti-activated Caspase-3 is commonly used a marker for apoptosis and has been used to detect apoptotic neuronal cells on cerebellar and retinal sections in mammals and zebrafish respectively (Van Hove et al., 2012b; Verslegers et al., 2013b; Bhumika et al., 2015). Alpha-tubulin has been reported to stain the optic nerve head, the nerve fiber layer (NFL) and the inner nuclear layer (INL) in the retina of developing and adult zebrafish (Fein et al., 2007; Diekmann et al., 2015). Stainings with the mouse anti-α-tubulin antibody, T9026, on retinal sections of adult zebrafish sections produced a similar staining pattern, thereby validating the use of this antibody as a marker for RGC axons. MAP2 is a microtubule associated protein commonly used to stain neuronal dendrites in the mammalian brain (Kosik and Finch, 1987). Moreover, its dendritic compartmentalization has been long confirmed in the rat retina, where is has been found expressed in RGC dendrites and other inner plexiform layer (IPL) neurites belonging to INL neurons (Okabe et al., 1989). Anti-MAP2 stainings on zebrafish retinal sections equally visualized IPL dendrites in the adult zebrafish retina, thus validating this antibody. The used anti-SV2 antibody has been included in the JCN antibody database and has been extensively characterized as a marker for synaptic vesicles in the adult zebrafish retina (ZDB-ATB-081201-1) (Yazulla and Studholme, 2001; Battista et al., 2009). For both IHC and WB, none of the observed staining patterns were caused by a non-specific binding of secondary antibodies since labeling with the used secondary antibodies alone did not yield

fluorescence on sections, nor bands on WB analysis. Negative controls were included in each experiment.

Retinal broad-spectrum MMP inhibition

To study the effect of broad-spectrum MMP inhibition on zebrafish retinotectal regeneration, the peptidyl hydroxamate inhibitor, GM6001 (Santa Cruz, sc-203979), and respective control solutions (Dimethylsulfoxide (DMSO)/PBS) were intravitreally injected using a micro-injector (UMP3, World Precision Instruments) at 1, 3, 4 and 6dpi. 300 nl of either used solution was injected over a 2-minute period to avoid reflux. GM6001 was dissolved in DMSO and injected at a 5 mM working concentration (10% DMSO), diluted in PBS, as described previously (Manabe et al., 2005). 10% DMSO and PBS injected eyes were taken as control. A minimum of 14 fish was treated with either DMSO or GM6001 and 8 fish were injected with PBS.

Visualization and quantification of optic tectum reinnervation

Regenerating axons from the retina towards the optic tectum (OT) were visualized by means of biocytin tracing as described previously (Becker et al., 1997; Becker et al., 2000). Briefly, fish were anesthetized (0,03% tricaine), the ON was transected between the ON head and crush site, and a small piece of gelfoam soaked in biocytin (Sigma Aldrich) was placed on the distal ON stump. The eye was placed back into its socket and fish were revived, allowing the tracer to be anterogradely transported towards the OT. After 3 h, fish were euthanized (0.1% tricaine) and transcardially perfused, first with PBS and then with a solution of 2% PFA and 2.5% glutaraldehyde in PBS. Brains were dissected and postfixed overnight in 4% PFA. After rinsing in PBS and embedding in 4% agarose (in PBS), 50 μm thick coronal vibratome sections were made. The biocytin signal was visualized by means of a Vectastain ABC kit (Vector laboraties), using DAB as a chromogen. Sections were dried on gelatin-coated slides and counterstained with neutral red solution to allow for brain nuclei identification. Brain sections through the central optic tectum (cross sections 168-179) were identified based on the presence of specific nuclei (Wullimann et al., 1996) and histological photographs were acquired with a microscope Zeiss imager Z1 at 10x magnification. Tectal reinnervation was analyzed by employing an in-house developed automated program designed with Image J software as previously reported (Bhumika et al., 2015). Briefly, the white matter of the OT was delineated, enabling the software to measure the whole region of

interest. Next, a threshold was set to measure the biocytin-labeled area within this target area. The ratio of both values provided the amount of tectal reinnervation per section. Of each fish, minimally 3 sections were analyzed and 8-15 fish were used per condition. Of note, in all experiments, uncrushed control (UCC) fish were included, of which OT reinnervation was analyzed and set as a 100% reference value. Reinnervation values obtained from the injury conditions were expressed in % relative to this reference control.

Statistical analysis

Comparison of western blot data from the sham-operated and crushed groups at a specific time-point post-injury was performed by an unpaired Student's *t*-test. For multiple group comparisons, analysis was done by one-way Anova followed by Tukey post hoc test on normalized data. Normal distribution was verified using a Kolmogorov-Smirnov test. All values are represented as mean ± SEM and $p < 0.05$ was considered statistically significant.

Results

Detailed characterization of the zebrafish ONC model

The zebrafish ONC model is a promising tool for the identification of new regenerative molecules. As such, a reasonable amount of studies already mapped the time-frame of axonal regeneration after ONC using different parameters. However, an all-in-one characterization of the ongoing processes seems to be lacking, thus impeding efficient research. Therefore, and to validate our ONC model, we first specifically studied retinal apoptosis and axonal regrowth in adult zebrafish subjected to ONC.

Optic nerve crush in zebrafish does not induce retinal apoptosis

To date, different observations regarding RGC apoptosis after ONC in zebrafish have been reported. Indeed, numbers vary from a negligible amount of apoptotic cells after ONC to a 20 % marked RGC death (Zhou and Wang, 2002; Zou et al., 2013). Immunostaining for activated Caspase-3 staining on retinal sections, harvested at 0, 1, 2 and 7 dpi, revealed no apoptotic cells over the entire retina (data not shown), thus indicating an absence of induced cell death in our ONC model.

Defining zebrafish optic nerve regeneration: Mapping retinal Gap-43 expression

Growth-associated protein 43 (GAP-43) is an established gene marker to define the four major phases of optic nerve regeneration after ONC in zebrafish, i.e. the injury response phase (< 1dpi), axonal outgrowth (1-7 dpi), axonal extension (5-18 dpi) and target contact and synaptic refinement phase (14-25 dpi) (McCurley and Callard, 2010). Indeed, real time qPCR and *in situ* hybridization repeatedly showed that *gap-43* is maximally upregulated in RGCs at 4 dpi, during axonal outgrowth, and afterwards gradually declines to reach baseline levels during synaptic refinement in the OT (Bormann et al., 1998; Udvadia et al., 2001; Becker and Becker, 2007a; McCurley and Callard, 2010). However, apart from one recently published article by Diekmann et al. (2015), data about Gap-43 expression at the protein level in the zebrafish retina after ONC are scarce. As such, to validate our model, we characterized the Gap-43 spatiotemporal expression pattern in the retina at several time points after ONC, through a combined use of WB and IHC. WB experiments indeed show a peak in Gap-43 protein expression (20-25 kDa) at 4 dpi, in accordance with published RT-qPCR data (Fig. 1A, B) (McCurley and Callard, 2010). Immunolabeling of retinal sections revealed a strong upregulation of Gap-43 in RGC somata and axons at 4 dpi, as compared to control fish, thereby suggesting increased Gap-43 production. At 7dpi, the Gap-43 signal seemed reduced in RGC somata, but was clearly still elevated in regrowing RGC axons (Fig. 1C). As Gap-43 is a membrane associated protein which is transported towards the growth cone, the observed IHC pattern at 7 dpi likely indicates an intracellular redistribution of Gap-43 in regenerating RGCs. At 14 dpi, towards the end of axonal extension, axonal Gap-43 expression re-approached baseline control levels (Fig. 1C). Of note, similar to what has been observed in Tg*(Gap-43:eGFP)* fish by Diekmann et al. (2015), our immunostainings also revealed Gap-43 expression in the IPL of naïve fish, which dispersed after ONC (Fig. 1C). Overall, the peak in retinal Gap-43 protein expression at 4 dpi and the clear presence of Gap-43 in RGC somata and intraretinal regrowing axons from 4-7 dpi are in line with previously published Gap-43 expression data, thereby validating our model (Diekmann et al., 2015).

Defining zebrafish optic nerve regeneration: Analysis of optic tectum (OT) reinnervation

Previous reports indicated that at 7 days post ONC, the majority of RGC axons is reinnervating the OT and thus 7 dpi forms an optimal time point to study the effect of drug application on retinotectal regeneration (Kaneda et al., 2008; Zou et al., 2013; Bhumika et al.,

2015). To verify this in our ONC model, axons were anterogradely traced with biocytin and axonal regeneration was measured at the level of the OT in uncrushed control (UCC) and crushed fish at 7 dpi. In the UCC condition, a punctuate pattern, representative for axon termini, can be noticed along the outer layers of the contralateral OT, i.e. the stratum opticum and stratum fibrosum et griseum superficial (Fig. 1D). In brains of crushed fish, individual axons entering the contralateral OT can clearly be distinguished at 7 dpi (Fig. 1D). As can be seen on the low magnification images, no axons were visualized in the ipsilateral OT, indicating an absence of axonal misguidance (Fig. 1D). Since the area covered by RGC axons in the OT of UCC fish can be considered maximal, UCC tectal innervation was set at 100% (Fig. 1E). Reinnervation at 7 dpi was calculated relative to the 100% UCC values. As only 66% of the OT was reinnervated at 7 dpi, RGC axons were clearly still regrowing at one week after crush, indeed allowing us to use this time-point for the evaluation of drug interference on OT reinnervation at 7dpi (Fig. 1E).

A role for MMPs in axonal regrowth during retinotectal regeneration

Inhibiting MMP functioning in the retina results in a reduced tectal reinnervation

Based on previous expression studies in lower vertebrates, a potential role of MMPs in CNS regeneration was suspected. To study the effect of overall MMP activity on retinotectal regeneration, GM6001, a broad-spectrum MMP inhibitor, was repeatedly injected intravitreally after ONC (1, 3, 4 and 6 dpi). Fish injected with DMSO served as control as this solvent was used to dissolve the inhibitor. However, it is more and more recognized that DMSO can cause neuronal damage and thus induce apoptosis, also after intravitreal injections (Hanslick et al., 2009; Galvao et al., 2014). As such, to assess for any possible toxic effects of repeated DMSO exposure, a group of fish injected with equal amounts (300 nl) of PBS was maintained alongside. At 7dpi, biocytin labeling was carried out and fish were sacrificed to analyze OT reinnervation. Similar to uninjected fish at 7 dpi, both DMSO and PBS injected fish showed about 60% OT reinnervation, as compared to UCCs. Also, no significant difference in the amount of regrowing axons was observed between the PBS and DMSO condition, indicating that the use of DMSO as a solvent in our experiments does not influence retinotectal regeneration (Fig. 2A, B). Notably, a clear reduction in OT reinnervation in fish treated with GM6001 can be seen compared to the two vehicle conditions (Fig. 2A). Semi-quantitative analysis indeed revealed a significant decrease in tectal reinnervation of 40% in

GM6001 treated fish compared to DMSO and PBS injected fish (Fig. 2B). Overall, these data suggest that lowering MMP activity in the retina after ONC negatively affects retinotectal regeneration.

RGC survival and retinal thickness are unaffected by repeated intravitreal GM6001 injections

Multiple studies have implicated MMPs as potential regulators of neuronal apoptosis (Manabe et al., 2005; Rosenberg, 2009; Van Hove et al., 2012a). As such, to further investigate whether the reduced retinotectal regeneration after GM6001 treatment could be due to increased RGC apoptosis, an activated caspase-3 staining was performed on retinal sections of PBS, DMSO and GM6001 injected fish at 2dpi, thus at 1 day after the first intravitreal injection. Uninjected 2 dpi fish were included as an extra control. At 2dpi, no apoptotic cells were detected in the retina of uninjected or PBS, DMSO and GM6001 treated fish, as shown by representative images in figure 3A. Also, an equal amount of DAPI^{+} cells per 100 μm RGC layer was observed in all four conditions, confirming that early phase retinal broad-spectrum MMP inhibition does not induce retinal apoptosis after ONC (Fig. 3E). To further assess for possible toxic effects of repeated GM6001 treatment, apoptosis was evaluated in crushed retinas of PBS, DMSO and GM6001 treated fish at 7dpi, 1 day after the last injection time point. As expected, no apoptotic cells were detected in 7 dpi uninjected fish, which served as an extra control (Fig. 3C). Although apoptosis was also absent in the INL and outer nuclear layer (ONL), a few apoptotic cells in the retinal ganglion cell layer (RGCL) could be detected at 7 dpi in all three injected conditions (Fig. 3B, C). Yet, quantitative analysis did not reveal any difference in the percentage of apoptotic RGCs between PBS, DMSO and GM6001 injected zebrafish (Fig. 3D). Moreover, a similar number of DAPI^{+} cells per 100 μm RGC layer was found in all four conditions, (Fig. 3E), thereby excluding any possible necrotic or apoptotic effect of retinal neurons due to DMSO and/or broad-spectrum MMP inhibition. Furthermore, in comparison to all other conditions, GM6001 injected fish did not show any obvious disruption of retinal morphology (Fig. 3C), nor a decrease in retinal thickness after ONC (Fig. 3F), again confirming the absence of toxic GM6001 levels.

Determination of the MMP spatiotemporal expression pattern after ONC

Our functional data with MMP inhibition, together with a recent transcriptome profiling study on zebrafish eyes after ONC (McCurley and Callard, 2010), suggest MMPs as important players in zebrafish retinotectal regeneration. Therefore, we decided to accurately determine the retinal spatiotemporal expression pattern of Mmp-13a, -2, -14 and -9 protein after ONC in adult zebrafish. This with the goal to specifically ascribe a potential role for each studied MMP in zebrafish retinotectal regeneration and to bring forward the most likely MMP affecting RGC axonal regrowth after ONC.

Increased expression of active Mmp-13a in RGC somata and primary dendrites during axonal regrowth

Using a primary antibody specifically developed to detect the Mmp-13a isoform in zebrafish (Anaspec, AS-55114), we determined the retinal spatiotemporal expression pattern for Mmp-13a protein in adult zebrafish after ONC. Western blot experiments, performed on retinal samples at various time points post ONC, showed a prominent rise in retinal active Mmp-13a (45 kDa) after ONC, compared to sham-operated fish, with a significant peak around 7 dpi, followed by a steep decrease towards control values at 14 dpi (Fig. 4A, B). No difference in pro Mmp-13a (80 kDa) was observed throughout regeneration (Fig. 4A). Fluorescent immunostainings for Mmp-13a revealed a weak Mmp-13a immunoreactivity in the RGCL and INL at 0dpi. An elevated Mmp-13a signal could be seen in the RGCL at 7dpi. At 14 dpi, Mmp-13a expression had again decreased, in accordance with the obtained WB data (Fig. 4C). At a higher magnification, the Mmp-13a signal was found to be confined to the RGC cytoplasm, as confirmed by H&E staining and light microscopic DAB staining for Mmp-13a on adjacent retinal sections (Fig. 4D). Furthermore, both DAB and fluorescent stainings depict Mmp-13a expression in the RGC primary dendrites (Fig. 4D). Our results thus clearly indicate a prominent retinal Mmp-13a upregulation throughout retinotectal regeneration. Notably, the peak in Mmp-13a protein around 7dpi, the time point at which RGC axonal outgrowth is fully ongoing, corresponds to a high Mmp-13a protein expression in RGC somata and primary dendrites.

Elevated presence of Mmp-2 in RGC somata and axons during axonal regeneration

To define the Mmp-2 spatiotemporal expression pattern in the retina after ONC, rabbit anti-MMP-2 (Santa Cruz, sc-8835-R) was used. Remarkably, after WB, only one protein band was detected within the 60-80 kDa range with this primary antibody in retinal protein samples. As such, as a positive control, we used lysates of zebrafish embryos at 30 hours post fertilization (hpf), known to express both pro- (72 kDa) and active Mmp-2 (64 kDa) (Janssens et al., 2013). Comparison to this positive control showed presence of active Mmp-2 in the adult zebrafish retina (Fig. 5A). Similar to Mmp-13a, yet with a delay of 3 days, active Mmp-2 was found to be upregulated in the retina during retinotectal regeneration. In detail, Mmp-2 expression augmented from 7 dpi, became 3 times higher compared to sham-operated fish at 10 dpi and finally re-approached control levels at 18 dpi (Fig. 5A, B). Immunostaining of retinal sections revealed that at 0 dpi and at all time points after ONC, Mmp-2 was localized in/on RGC axons (Fig. 5D), as shown by a double labeling for α-tubulin (Fig. 5C). However, shortly after ONC and until 4 dpi, Mmp-2 expression faded in RGC axons. Strikingly, from 4 dpi onwards, Mmp-2 expression became apparent in RGC somata, where it seemingly increased until 10 dpi. Moreover, at 7 and 10 dpi, Mmp-2 signal could again be visualized in regrowing RGC axons (Fig. 5D). At 14 dpi, during axonal extension, Mmp-2 expression was again found restricted to RGC axons only (Fig. 5D). Of note, consistent expression of Mmp-2 was also observed in the PRL in all conditions. Overall, the elevated expression of Mmp-2 in RGCs and its axons during axonal regrowth could be indicative for an important role of Mmp-2 in zebrafish retinotectal regeneration.

Biphasic expression pattern of Mmp-14 in the zebrafish retina during optic nerve regeneration

By using a commercially available and widely used polyclonal antibody for MMP-14 (Abcam, ab53712), we determined the spatiotemporal expression pattern of Mmp-14 in the zebrafish retina after ONC. MMP-14, or membrane-type 1 MMP, is one of the six membrane-bound MMPs, which are typically intracellularly activated in the Golgi complex prior to being tethered to the cell membrane (Mannello and Medda, 2012). In zebrafish, Mmp-14 is present at the cell surface as a 55-60 kDa active proteinase, also called 'mature Mmp-14'. A biphasic expression pattern for mature Mmp-14 could be detected. Indeed, after an initial peak in expression during the injury response phase (6hpi), retinal Mmp-14 gradually decreased during axonal regeneration, reaching its minimum at 10 dpi. Afterwards, Mmp-14 levels were

approximately restored to control values (Fig. 6A, B). To investigate the localization of Mmp-14 in the zebrafish retina, retinal sections were immunolabeled for Mmp-14 and double stained with α-tubulin and MAP2 (2a+2b), a marker for neuronal dendrites. On naive and sham-operated sections, Mmp-14 was abundantly expressed in/on RGC axons (Fig. 6E), but was also found in the IPL, where it appeared in a patchy pattern (Fig. 6C). A more detailed confocal z-stack picture of the IPL and double staining with MAP2, revealed Mmp-14 expression in IPL neurites (Fig. 6D). When analyzing immunostainings on retinal sections after ONC, the fluctuating expression pattern, which was found with WB, was confirmed. The Mmp-14 signal was clearly upregulated at 6 hpi, both in the NFL and IPL, and especially decreased in RGC axons during axonal regrowth (Fig. 6C). Consequently, a promoting function for Mmp-14 in axonal regrowth seems unlikely, but based on its expression pattern, a contributory role for this protease in neurite maintenance can be suspected.

Increased Mmp-9 expression in inner retinal synapses during retinotectal regeneration

The retinal spatiotemporal expression after ONC was also studied for Mmp-9. Similar to Mmp-2, after WB, only one protein band was detected with the Mmp-9 Ab (Anaspec, AS-55345) in adult retinal samples. As such, protein lysates of 5 days old zebrafish embryos were used as a positive control (see datasheet AS-55345 of the antibody providing company Anaspec). Figure 7A shows a perfect aligning of the retinal protein band with active Mmp-9 (76 kDa) in the positive control, thereby confirming the presence of active Mmp-9 in the adult zebrafish retina. After ONC, active Mmp-9 expression slowly increased and eventually became twice as high in the retina at 14dpi compared to sham-operated controls. At 3 weeks post-injury, Mmp-9 levels were restored to the control situation (Fig. 7A, B). IHC stainings localized Mmp-9 in the inner (IPL) and outer plexiform layer (OPL) of control retinas. In the IPL, 3 prominent strata were labeled, in which several puncta could be distinguished, suggestive for expression of Mmp-9 in synapses (Fig. 7C). Indeed, a double staining with the general synapse marker SV2 shows partial overlap with Mmp-9, thus revealing localization of Mmp-9 in a subset of IPL synapses (Fig. 7D). After ONC, the Mmp-9 signal became more abundant in the IPL, but not in the OPL, with a maximal presence at 14dpi, thereby confirming the WB data (Fig. 7C). As such, Mmp-9 might have a role in synaptic plasticity or growth in the regenerating adult zebrafish retina.

Discussion

Here, we provide primary evidence that *in vivo* retinal broad-spectrum MMP inhibition after ONC dramatically deteriorates axonal regeneration, thereby indicating a stimulatory role for MMPs in zebrafish RGC axonal regrowth. Moreover, we report a distinct regulation of MMP expression in RGC axons, somata and primary dendrites, and IPL neurites and synapses throughout zebrafish retinotectal regeneration after ONC, confirming MMP implication in axonal regrowth and inner retina remodeling.

To facilitate the interpretation of potential functional roles of MMPs in zebrafish retinotectal regeneration, we first mapped some important parameters of the ONC model. In agreement with recent findings of Zou et al. (2013), we report that most RGCs typically survive an ONC and seem to turn into a growth active state. Furthermore, our data agree with a recent paper describing spatiotemporal Gap-43 expression after ONC in Tg*(Gap-43:eGFP)* zebrafish (Diekmann et al., 2015), and reveal an increased Gap-43 immunoreactivity in RGC somata and axons during axonal regrowth (4-7 dpi). Also our WB data are in line with existing mRNA and *in situ* hybridization data which equally report an elevated expression of Gap-43 at 4 dpi after ONC, defined as the axonal outgrowth phase (McCurley and Callard, 2010). Moreover, the observation that zebrafish show only 60% OT reinnervation at 7 dpi compared to UCCs, confirmed that RGC axonal regrowth is fully ongoing in our ONC model at 1 week post-injury, which is in accordance with previous publications (Kaneda et al., 2008; Zou et al., 2013; Bhumika et al., 2015).

A former transcriptome profiling study showed a stringent correlation between the gene expression of four specific MMPs and the different regenerative phases after ONC, suggestive for a role of MMPs in zebrafish retinotectal regeneration (McCurley and Callard, 2010). Indeed, *in vivo* retinal broad-spectrum MMP inhibition after ONC by intravitreal injections of GM6001 significantly reduced the reinnervation of the OT by RGC axons with 40% at one week after injury compared to vehicle injected control fish. Since use of low concentrations of various MMP inhibitors on developing *Xenopus* RGCs was reported to result in axonal navigation defects, it was suggested that different MMPs may regulate axon behavior at distinct decision points (Webber et al., 2002; Hehr et al., 2005). Notably, here no new axons were detected in the ipsilateral optic tectum, thereby partly discarding axonal misnavigation as an explanation for the decreased amount of RGC axons present in the contralateral OT. Moreover, no effects of MMP inhibition were seen on RGC survival and

retinal thickness, thereby excluding toxic effects of the used compound and a general involvement of MMPs in apoptosis. Of note, the minutely amount of apoptosis which could be observed at 7 dpi after any treatment is probably caused by repeated intravitreal injections. However, we assume this does not influence the credibility of our experiments since no significant difference in the amount of DAPI$^+$ cells / 100 μm was detected between all conditions. Overall, our data implicate MMPs in actual RGC axonal regrowth/elongation after ONC in adult zebrafish. This observation is in accordance with other functional studies suggesting a role for MMPs in axonal outgrowth/extension in developing lower vertebrates. For example, application of GM6001 in the medium of zebrafish embryos resulted in a decreased OT innervation (Janssens et al., 2013). In addition, a diminished RGC axonal outgrowth was also observed in *Xenopus laevis* embryos after large dose broad-spectrum MMP inhibition (Webber et al., 2002). Furthermore, recently, broad-spectrum MMP inhibition has been shown to reduce axonal outgrowth of developing RGCs in an *ex vivo* mouse retinal explant model (Gaublomme et al., 2014).

Based on our data implying a regulatory role for MMPs in zebrafish retinotectal regeneration, and on a recent transcriptome profiling study on zebrafish eyes after ONC (McCurley and Callard, 2010), we decided to profoundly determine the spatiotemporal expression pattern of Mmp-2, 9, -13a and -14 in the zebrafish retina after ONC at the protein level. As depicted in Table 2, our protein expression data mostly confirm the patterns of RNA upregulation as reported by McCurley and Callard (2010), yet a general time shift in expression can be noticed. This should not come as a surprise since eukaryotic transcription and translation are separated in time and protein translation is highly subject to different cellular processes. More surprisingly is the observation that Mmp-14, seemingly upregulated at RNA level during regeneration, becomes, apart from a short peak during the injury response, significantly less expressed at protein level at later stages after ONC, as compared to sham-operated controls. Also here, one must keep in mind that protein abundances are determined by a balance in regulation of both RNA and protein production and turnover, thus making it sometimes hard to correlate RNA and protein expression levels (Vogel and Marcotte, 2012). Furthermore, our procedure only applied retinal extracts to analyze protein expression, while McCurley and Callard (2010) used entire eye samples to perform their transcriptome profiling study.

Combined interpretation of WB and IHC data revealed a prominent rise of active Mmp-13a in RGC somata and primary dendrites during RGC axonal regrowth after ONC. To

our knowledge, no data are available concerning the localization of Mmp-13a or possible functions of this collagenase in developing or adult zebrafish neuronal tissue. Apart from a role in wound healing through expression in subretinal macrophages in a murine model of retinal detachment, potential roles and expression data for MMP-13 in the mammalian visual system also seem inexistent (Kim et al., 2014). Considering the intraneuronal localization of Mmp-13a in zebrafish retina, a strong nuclear and cytoplasmic MMP-13 immunoreactivity has also been observed in neurons of both normal and ischemic rat and human brains (Nagel et al., 2005; Cuadrado et al., 2009). Based on the early time point of upregulation of MMP-13, both studies ascribed a potential damaging or apoptotic role to this proteinase. Besides, as cerebral ischemia in rats can trigger neurogenesis and MMP-13 was found expressed in a subset of proliferative neurons of the infracted region, a potential neurogenerative role for MMP-13 was also addressed (Nagel et al., 2005). However, as RGC apoptosis and neuronal proliferation are not induced in the zebrafish retina after ONC (Zou et al., 2013), the exact role of Mmp-13a during zebrafish retinotectal regeneration remains open for speculation. Although a neuroprotective role cannot be excluded, the time point (7 dpi) and localization (RGC cytoplasm/primary dendrite) of Mmp-13a upregulation, suggest a role for this MMP in RGC axonal regrowth or dendritic remodeling. Indeed, dendritic retraction/remodeling in the mammalian CNS as a response to stress or injury has been frequently described (Vyas et al., 2002; Weber and Harman, 2008; Kalesnykas et al., 2012). Moreover, dendritic remodeling of severed *Drosophila* sensory neurons seemingly requires MMPs (Kuo et al., 2005), as does activity dependent hippocampal dendritic remodeling in adult rats (Szklarczyk et al., 2002). Yet, the occurrence of dendritic remodeling after ONC in zebrafish appears unstudied. More specifically, Mmp-13a could function as a cell autonomous regulator of axonal regrowth and dendritic remodeling, or it could apply its cleaving capacities to activate other molecules/enzymes essential for axonal regrowth or dendritic remodeling. For example, in mammals it has been repeatedly reported that MMP-13 can activate MMP-2 and -9, two MMPs which are respectively upregulated in RGC somata/axons and synapses during zebrafish retinotectal regeneration (Pivetta et al., 2011; Kim et al., 2014).

Mmp-2 was found to be upregulated in growth-active RGCs and regrowing axons after ONC in adult zebrafish, similar to previously observed expression patterns in uninjured adult and developing vertebrate eyes. Indeed, expression of MMP-2 in RGCs and their axons has already been reported in adult naive human and monkey eyes and in outgrowing axons of ex vivo mouse retinal explants and developing zebrafish embryos (Agapova et al., 2001; Limb et

al., 2002; Agapova et al., 2003; Janssens et al., 2013; Gaublomme et al., 2014). Moreover, the latter two studies suggested a functional involvement of MMP-2 in RGC axonal outgrowth as the respective use of MMP-2 inhibitors and morpholinos prevented RGCs to effectively grow their axons. In adult mammals in which regeneration was triggered after injury of the spinal cord or optic nerve, a positive correlation between gelatinase activity and axonal regeneration has been observed, although causality was not demonstrated (Duchossoy et al., 2001a; Duchossoy et al., 2001b; Ahmed et al., 2005). Strikingly however, MMP-2 seemed mainly localized around the scar tissue itself. These studies then also suggest a role for MMP-2 in the breakdown of inhibitory molecules, e.g. CSPGs, thereby clearing the pathway along which neurites can regrow. In addition, it was shown that MMP-2 secreted by olfactory ensheating cells may contribute to axonal regeneration of cultured adult rat RGCs via degradation of CSPGs in scar tissue or local inhibitory ECM surrounding neuronal cell bodies (Pastrana et al., 2006). This is opposite to the situation during development, where a glial scar is absent and MMP-2 is suggested to have a direct role in axonal outgrowth (Gaublomme et al., 2014). Importantly, it is increasingly acknowledged that the CNS injury site in adult zebrafish shows little scarring and expression of inhibitory molecules (Becker and Becker, 2014). Also in our ONC model, no particular expression of Mmp-2 in astrocytes around the crush site was observed (data not shown). As such, the confined expression of Mmp-2 to regenerative RGC somata and its axons after ONC, suggests a promoting role for Mmp-2 in zebrafish retinotectal regeneration with actions intrinsic to RGC axonal regrowth.

Alike Mmp-2, Mmp-14 was also detected in RGC axons. Furthermore, Mmp-14 seemed present in IPL neurites of the adult zebrafish retina. Expression of MMP-14 has been previously reported in the optic nerve and IPL in developing zebrafish and in the NFL of postnatal mouse and adult monkey retinas (Agapova et al., 2003; Gariano et al., 2006; Janssens et al., 2013). A rather unconventional spatiotemporal expression pattern was noted for Mmp-14 in the adult zebrafish retina after ONC. Indeed, after an initial rise of mature Mmp-14 in RGC axons and IPL neurites during the injury response, its signal quickly decreased and reached a bottom level of only 20% expression compared to controls during the axonal regeneration phase. These data then also debunk a stimulatory role for Mmp-14 in axonal regrowth, which stands in sharp contrast with previously published papers ascribing an involvement of this enzyme in RGC axonal outgrowth of developing vertebrates. Indeed, knockdown of *mmp-14* in developing zebrafish embryos resulted in a reduced tectal innervation area, suggestive for an (in)direct effect of Mmp-14 on axonal outgrowth or

navigation (Janssens et al., 2013). Likewise, MMP-14 was shown to promote RGC axon outgrowth in the postnatal mouse retina through activation of MMP-2 as administration of an antibody that blocks the MMP-2 activating capacity of MMP-14 (mAb 9E8), significantly reduced neurite outgrowth (Gaublomme et al., 2014). However, nerve regeneration is not just a recapitulation of development and some genes can be differently regulated (Becker and Becker, 2014). Indeed, inhibition of MMP-14 activity after sciatic nerve crush in adult rats, enhanced axonal regrowth by promoting intraganglionic expression of regeneration associated genes (*Gap-43* and *Atf3*) and by preventing degradation of growth-permissive laminin (Nishihara et al., 2015). Based on this publication and as axonal regrowth fluently occurs in zebrafish after ONC, we hypothesize that Mmp-14 activity is autonomously downregulated during retinotectal regeneration to prevent destructive actions of this protease. On the other hand, the constitutive expression of Mmp-14 in RGC axons and IPL neurites and its reappearance during finalization of regeneration, might also implicate Mmp-14 in the maintenance of neurite integrity. As such, the short peak of mature Mmp-14 immediately after injury, could represent an attempt to retain the original neurite structure.

In case of Mmp-9, our data indicate an elevated expression in IPL synapses after ONC at the initiation of target contact and synaptic refinement in the OT. As such, as a response to RGCs re-establishing synaptic contacts with their target neurons in the optic tectum, synaptic plasticity might be induced in the retina itself. Consequently, Mmp-9 could be involved in synaptic plasticity or regrowth in the regenerating zebrafish retina, a process not yet examined. This finding would be in accordance with the wide range of results that imply MMPs, and MMP-9 in particular, as primordial players in hippocampal plasticity and reactive synaptogenesis after injury in the adult mammalian brain (Ethell and Ethell, 2007; Verslegers et al., 2013a; Phillips et al., 2014; Tsilibary et al., 2014).

In summary, this report confirmed the absence of RGC apoptosis and the time frame of axonal regeneration in adult zebrafish after ONC, in accordance with previous publications. Broad-spectrum MMP inhibition in the zebrafish retina through intravitreal injections of GM6001, provides novel *in vivo* evidence for a contributory role of MMPs in RGC axonal regrowth. In accordance, this study revealed dynamic expression patterns of specific MMPs in the injured zebrafish retina, suggestive for a promoting role for Mmp-13a and Mmp-2 in axonal regrowth and an inhibitory function for Mmp-14 in this process. In addition, Mmp-13a, -14 and -9 might be involved in inner retina remodeling. Of note, our experiments were designed in a way to characterize MMP expression and functioning primarily at the level of

the retina. Considering this on top of the strongly reduced inhibitory environment in zebrafish, our data are warily suggestive for an alternative way MMPs can promote axonal regeneration besides their previously suggested role in glial scar reduction, reported in various mammalian studies. Nonetheless, several questions concerning the individual functions of these MMPs remain. As such, future studies should focus on determining the exact role of specific MMPs in zebrafish retinotectal regeneration in order to unravel new molecular mechanisms underlying successful CNS regeneration.

Acknowledgements

Conflict of interest statement

The authors have no conflict of interest.

Role of authors

All authors had full access to all the data in the study and take responsibility for the integrity of the data and the accuracy of the data analysis. Study concept and design: KL, LM. Acquisition of data: KL, IB, SB. Analysis and interpretation of data: KL, IB, JVH. Drafting of the manuscript: KL. Critical revision of the manuscript for important intellectual content: IVH, LDG, LM, VMD. Statistical analysis: KL, IB. Obtained funding: KL, JVH, IVH (IWT), IB (FWO). Study supervision: VMD, LM.

References

Agapova OA, Kaufman PL, Lucarelli MJ, Gabelt BT, Hernandez MR. 2003. Differential expression of matrix metalloproteinases in monkey eyes with experimental glaucoma or optic nerve transection. Brain research 967(1-2):132-143.

Agapova OA, Ricard CS, Salvador-Silva M, Hernandez MR. 2001. Expression of matrix metalloproteinases and tissue inhibitors of metalloproteinases in human optic nerve head astrocytes. Glia 33(3):205-216.

Agrawal SM, Lau L, Yong VW. 2008. MMPs in the central nervous system: where the good guys go bad. Seminars in cell & developmental biology 19(1):42-51.

Ahmed Z, Dent RG, Leadbeater WE, Smith C, Berry M, Logan A. 2005. Matrix metalloproteases: degradation of the inhibitory environment of the transected optic nerve and the scar by regenerating axons. Molecular and cellular neurosciences 28(1):64-78.

Battista AG, Ricatti MJ, Pafundo DE, Gautier MA, Faillace MP. 2009. Extracellular ADP regulates lesion-induced in vivo cell proliferation and death in the zebrafish retina. Journal of neurochemistry 111(2):600-613.

Becker CG, Becker T. 2007a. Growth and pathfinding of regenerating axons in the optic projection of adult fish. Journal of neuroscience research 85(12):2793-2799.

Becker CG, Becker T. 2007b. Model organisms in spinal cord regeneration. Weinheim: Wiley-VCH.

Becker CG, Becker T. 2008. Adult zebrafish as a model for successful central nervous system regeneration. Restorative neurology and neuroscience 26(2-3):71-80.

Becker CG, Meyer RL, Becker T. 2000. Gradients of ephrin-A2 and ephrin-A5b mRNA during retinotopic regeneration of the optic projection in adult zebrafish. The Journal of comparative neurology 427(3):469-483.

Becker T, Becker CG. 2014. Axonal regeneration in zebrafish. Current opinion in neurobiology 27:186-191.

Becker T, Wullimann MF, Becker CG, Bernhardt RR, Schachner M. 1997. Axonal regrowth after spinal cord transection in adult zebrafish. The Journal of comparative neurology 377(4):577-595.

Benowitz LI, Popovich PG. 2011. Inflammation and axon regeneration. Current opinion in neurology 24(6):577-583.

Benowitz LI, Yin Y. 2007. Combinatorial treatments for promoting axon regeneration in the CNS: strategies for overcoming inhibitory signals and activating neurons' intrinsic growth state. Developmental neurobiology 67(9):1148-1165.

Berry M, Ahmed Z, Lorber B, Douglas M, Logan A. 2008. Regeneration of axons in the visual system. Restorative neurology and neuroscience 26(2-3):147-174.

Bhumika S, Lemmens K, Vancamp P, Moons L, Darras VM. 2015. Decreased thyroid hormone signaling accelerates the reinnervation of the optic tectum following optic nerve crush in adult zebrafish. Molecular and cellular neurosciences 68:92-102.

Bormann P, Zumsteg VM, Roth LW, Reinhard E. 1998. Target contact regulates GAP-43 and alpha-tubulin mRNA levels in regenerating retinal ganglion cells. Journal of neuroscience research 52(4):405-419.

Cauwe B, Opdenakker G. 2010. Intracellular substrate cleavage: a novel dimension in the biochemistry, biology and pathology of matrix metalloproteinases. Critical reviews in biochemistry and molecular biology 45(5):351-423.

Cerveny KL, Varga M, Wilson SW. 2012. Continued growth and circuit building in the anamniote visual system. Developmental neurobiology 72(3):328-345.

Chernoff EA. 1996. Spinal cord regeneration: a phenomenon unique to urodeles? The International journal of developmental biology 40(4):823-831.

Chernoff EA, O'Hara CM, Bauerle D, Bowling M. 2000. Matrix metalloproteinase production in regenerating axolotl spinal cord. Wound repair and regeneration : official publication of the Wound Healing Society [and] the European Tissue Repair Society 8(4):282-291.

Cua RC, Lau LW, Keough MB, Midha R, Apte SS, Yong VW. 2013. Overcoming neurite-inhibitory chondroitin sulfate proteoglycans in the astrocyte matrix. Glia 61(6):972-984.

Cuadrado E, Rosell A, Borrell-Pages M, Garcia-Bonilla L, Hernandez-Guillamon M, Ortega-Aznar A, Montaner J. 2009. Matrix metalloproteinase-13 is activated and is found in the nucleus of neural cells after cerebral ischemia. Journal of cerebral blood flow and metabolism : official journal of the International Society of Cerebral Blood Flow and Metabolism 29(2):398-410.

de Lima S, Habboub G, Benowitz LI. 2012. Combinatorial therapy stimulates long-distance regeneration, target reinnervation, and partial recovery of vision after optic nerve injury in mice. International review of neurobiology 106:153-172.

Diekmann H, Kalbhen P, Fischer D. 2015. Characterization of optic nerve regeneration using transgenic zebrafish. Frontiers in cellular neuroscience 9:118.

Duchossoy Y, Arnaud S, Feldblum S. 2001a. Matrix metalloproteinases: potential therapeutic target in spinal cord injury. Clinical chemistry and laboratory medicine : CCLM / FESCC 39(4):362-367.

Duchossoy Y, Horvat JC, Stettler O. 2001b. MMP-related gelatinase activity is strongly induced in scar tissue of injured adult spinal cord and forms pathways for ingrowing neurites. Molecular and cellular neurosciences 17(6):945-956.

Elsaeidi F, Bemben MA, Zhao XF, Goldman D. 2014. Jak/Stat signaling stimulates zebrafish optic nerve regeneration and overcomes the inhibitory actions of Socs3 and Sfpq. The Journal of neuroscience : the official journal of the Society for Neuroscience 34(7):2632-2644.

Ethell IM, Ethell DW. 2007. Matrix metalloproteinases in brain development and remodeling: synaptic functions and targets. Journal of neuroscience research 85(13):2813-2823.

Fein AJ, Meadows LS, Chen C, Slat EA, Isom LL. 2007. Cloning and expression of a zebrafish SCN1B ortholog and identification of a species-specific splice variant. BMC genomics 8:226.

Filous AR, Miller JH, Coulson-Thomas YM, Horn KP, Alilain WJ, Silver J. 2010. Immature astrocytes promote CNS axonal regeneration when combined with chondroitinase ABC. Developmental neurobiology 70(12):826-841.

Fleisch VC, Fraser B, Allison WT. 2011. Investigating regeneration and functional integration of CNS neurons: lessons from zebrafish genetics and other fish species. Biochimica et biophysica acta 1812(3):364-380.

Gallego BI, Salazar JJ, de Hoz R, Rojas B, Ramirez AI, Salinas-Navarro M, Ortin-Martinez A, Valiente-Soriano FJ, Aviles-Trigueros M, Villegas-Perez MP, Vidal-Sanz M, Trivino A, Ramirez JM. 2012. IOP induces upregulation of GFAP and MHC-II and microglia reactivity in mice retina contralateral to experimental glaucoma. Journal of neuroinflammation 9:92.

Galvao J, Davis B, Tilley M, Normando E, Duchen MR, Cordeiro MF. 2014. Unexpected low-dose toxicity of the universal solvent DMSO. FASEB journal : official publication of the Federation of American Societies for Experimental Biology 28(3):1317-1330.

Gariano RF, Hu D, Helms J. 2006. Expression of angiogenesis-related genes during retinal development. Gene expression patterns : GEP 6(2):187-192.

Gaublomme D, Buyens T, De Groef L, Stakenborg M, Janssens E, Ingvarsen S, Porse A, Behrendt N, Moons L. 2014. Matrix metalloproteinase 2 and membrane type 1 matrix metalloproteinase co-regulate axonal outgrowth of mouse retinal ganglion cells. Journal of neurochemistry 129(6):966-979.

Hanslick JL, Lau K, Noguchi KK, Olney JW, Zorumski CF, Mennerick S, Farber NB. 2009. Dimethyl sulfoxide (DMSO) produces widespread apoptosis in the developing central nervous system. Neurobiology of disease 34(1):1-10.

Hehr CL, Hocking JC, McFarlane S. 2005. Matrix metalloproteinases are required for retinal ganglion cell axon guidance at select decision points. Development 132(15):3371-3379.

Horner PJ, Gage FH. 2000. Regenerating the damaged central nervous system. Nature 407(6807):963-970.

Hsu JY, McKeon R, Goussev S, Werb Z, Lee JU, Trivedi A, Noble-Haeusslein LJ. 2006. Matrix metalloproteinase-2 facilitates wound healing events that promote functional recovery after spinal cord injury. The Journal of neuroscience : the official journal of the Society for Neuroscience 26(39):9841-9850.

Huebner EA, Strittmatter SM. 2009. Axon regeneration in the peripheral and central nervous systems. Results and problems in cell differentiation 48:339-351.

Janssens E, Gaublomme D, De Groef L, Darras VM, Arckens L, Delorme N, Claes F, Van Hove I, Moons L. 2013. Matrix metalloproteinase 14 in the zebrafish: an eye on retinal and retinotectal development. PloS one 8(1):e52915.

Kalesnykas G, Oglesby EN, Zack DJ, Cone FE, Steinhart MR, Tian J, Pease ME, Quigley HA. 2012. Retinal ganglion cell morphology after optic nerve crush and experimental glaucoma. Investigative ophthalmology & visual science 53(7):3847-3857.

Kaneda M, Nagashima M, Nunome T, Muramatsu T, Yamada Y, Kubo M, Muramoto K, Matsukawa T, Koriyama Y, Sugitani K, Vachkov IH, Mawatari K, Kato S. 2008. Changes of phospho-growth-

associated protein 43 (phospho-GAP43) in the zebrafish retina after optic nerve injury: a long-term observation. Neuroscience research 61(3):281-288.

Kapfhammer JP, Christ F, Schwab ME. 1997. The growth-associated protein GAP-43 is specifically expressed in tyrosine hydroxylase-positive cells of the rat retina. Brain research Developmental brain research 101(1-2):257-264.

Kim B, Abdel-Rahman MH, Wang T, Pouly S, Mahmoud AM, Cebulla CM. 2014. Retinal MMP-12, MMP-13, TIMP-1, and TIMP-2 expression in murine experimental retinal detachment. Investigative ophthalmology & visual science 55(4):2031-2040.

Kosik KS, Finch EA. 1987. MAP2 and tau segregate into dendritic and axonal domains after the elaboration of morphologically distinct neurites: an immunocytochemical study of cultured rat cerebrum. The Journal of neuroscience : the official journal of the Society for Neuroscience 7(10):3142-3153.

Kuo CT, Jan LY, Jan YN. 2005. Dendrite-specific remodeling of Drosophila sensory neurons requires matrix metalloproteases, ubiquitin-proteasome, and ecdysone signaling. Proceedings of the National Academy of Sciences of the United States of America 102(42):15230-15235.

Kurimoto T, Yin Y, Habboub G, Gilbert HY, Li Y, Nakao S, Hafezi-Moghadam A, Benowitz LI. 2013. Neutrophils express oncomodulin and promote optic nerve regeneration. The Journal of neuroscience : the official journal of the Society for Neuroscience 33(37):14816-14824.

Kurimoto T, Yin Y, Omura K, Gilbert HY, Kim D, Cen LP, Moko L, Kugler S, Benowitz LI. 2010. Long-distance axon regeneration in the mature optic nerve: contributions of oncomodulin, cAMP, and pten gene deletion. The Journal of neuroscience : the official journal of the Society for Neuroscience 30(46):15654-15663.

Li R, Shen Y. 2013. An old method facing a new challenge: re-visiting housekeeping proteins as internal reference control for neuroscience research. Life sciences 92(13):747-751.

Limb GA, Daniels JT, Pleass R, Charteris DG, Luthert PJ, Khaw PT. 2002. Differential expression of matrix metalloproteinases 2 and 9 by glial Muller cells: response to soluble and extracellular matrix-bound tumor necrosis factor-alpha. The American journal of pathology 160(5):1847-1855.

Lorber B, Guidi A, Fawcett JW, Martin KR. 2012. Activated retinal glia mediated axon regeneration in experimental glaucoma. Neurobiology of disease 45(1):243-252.

Manabe S, Gu Z, Lipton SA. 2005. Activation of matrix metalloproteinase-9 via neuronal nitric oxide synthase contributes to NMDA-induced retinal ganglion cell death. Investigative ophthalmology & visual science 46(12):4747-4753.

Mannello F, Medda V. 2012. Nuclear localization of matrix metalloproteinases. Progress in histochemistry and cytochemistry 47(1):27-58.

McCurley AT, Callard GV. 2010. Time Course Analysis of Gene Expression Patterns in Zebrafish Eye During Optic Nerve Regeneration. Journal of experimental neuroscience 2010(4):17-33.

Morrison CJ, Butler GS, Rodriguez D, Overall CM. 2009. Matrix metalloproteinase proteomics: substrates, targets, and therapy. Current opinion in cell biology 21(5):645-653.

Nagase H, Visse R, Murphy G. 2006. Structure and function of matrix metalloproteinases and TIMPs. Cardiovascular research 69(3):562-573.

Nagel S, Sandy JD, Meyding-Lamade U, Schwark C, Bartsch JW, Wagner S. 2005. Focal cerebral ischemia induces changes in both MMP-13 and aggrecan around individual neurons. Brain research 1056(1):43-50.

Neve LD, Savage AA, Koke JR, Garcia DM. 2012. Activating transcription factor 3 and reactive astrocytes following optic nerve injury in zebrafish. Comparative biochemistry and physiology Toxicology & pharmacology : CBP 155(2):213-218.

Nishihara T, Remacle AG, Angert M, Shubayev I, Shiryaev SA, Liu H, Dolkas J, Chernov AV, Strongin AY, Shubayev VI. 2015. Matrix metalloproteinase-14 both sheds cell surface neuronal glial antigen 2 (NG2) proteoglycan on macrophages and governs the response to peripheral nerve injury. The Journal of biological chemistry 290(6):3693-3707.

Okabe S, Shiomura Y, Hirokawa N. 1989. Immunocytochemical localization of microtubule-associated proteins 1A and 2 in the rat retina. Brain research 483(2):335-346.

Page-McCaw A, Ewald AJ, Werb Z. 2007. Matrix metalloproteinases and the regulation of tissue remodelling. Nature reviews Molecular cell biology 8(3):221-233.

Pastrana E, Moreno-Flores MT, Gurzov EN, Avila J, Wandosell F, Diaz-Nido J. 2006. Genes associated with adult axon regeneration promoted by olfactory ensheathing cells: a new role for matrix metalloproteinase 2. The Journal of neuroscience : the official journal of the Society for Neuroscience 26(20):5347-5359.

Petrey AC, Flanagan-Steet H, Johnson S, Fan X, De la Rosa M, Haskins ME, Nairn AV, Moremen KW, Steet R. 2012. Excessive activity of cathepsin K is associated with cartilage defects in a zebrafish model of mucolipidosis II. Disease models & mechanisms 5(2):177-190.

Phillips LL, Chan JL, Doperalski AE, Reeves TM. 2014. Time dependent integration of matrix metalloproteinases and their targeted substrates directs axonal sprouting and synaptogenesis following central nervous system injury. Neural regeneration research 9(4):362-376.

Pivetta E, Scapolan M, Pecolo M, Wassermann B, Abu-Rumeileh I, Balestreri L, Borsatti E, Tripodo C, Colombatti A, Spessotto P. 2011. MMP-13 stimulates osteoclast differentiation and activation in tumour breast bone metastases. Breast cancer research : BCR 13(5):R105.

Rosenberg GA. 2009. Matrix metalloproteinases and their multiple roles in neurodegenerative diseases. Lancet neurology 8(2):205-216.

Sternlicht MD, Werb Z. 2001. How matrix metalloproteinases regulate cell behavior. Annual review of cell and developmental biology 17:463-516.

Szklarczyk A, Lapinska J, Rylski M, McKay RD, Kaczmarek L. 2002. Matrix metalloproteinase-9 undergoes expression and activation during dendritic remodeling in adult hippocampus. The Journal of neuroscience : the official journal of the Society for Neuroscience 22(3):920-930.

Tsilibary E, Tzinia A, Radenovic L, Stamenkovic V, Lebitko T, Mucha M, Pawlak R, Frischknecht R, Kaczmarek L. 2014. Neural ECM proteases in learning and synaptic plasticity. Progress in brain research 214:135-157.

Udvadia AJ, Koster RW, Skene JH. 2001. GAP-43 promoter elements in transgenic zebrafish reveal a difference in signals for axon growth during CNS development and regeneration. Development 128(7):1175-1182.

Van Hove I, Lemmens K, Van de Velde S, Verslegers M, Moons L. 2012a. Matrix metalloproteinase-3 in the central nervous system: a look on the bright side. Journal of neurochemistry 123(2):203-216.

Van Hove I, Verslegers M, Buyens T, Delorme N, Lemmens K, Stroobants S, Gantois I, D'Hooge R, Moons L. 2012b. An aberrant cerebellar development in mice lacking matrix metalloproteinase-3. Molecular neurobiology 45(1):17-29.

Veeravalli KK, Dasari VR, Tsung AJ, Dinh DH, Gujrati M, Fassett D, Rao JS. 2009. Human umbilical cord blood stem cells upregulate matrix metalloproteinase-2 in rats after spinal cord injury. Neurobiology of disease 36(1):200-212.

Verslegers M, Lemmens K, Van Hove I, Moons L. 2013a. Matrix metalloproteinase-2 and -9 as promising benefactors in development, plasticity and repair of the nervous system. Progress in neurobiology 105:60-78.

Verslegers M, Van Hove I, Buyens T, Dekeyster E, Knevels E, Moons L. 2013b. Identification of MMP-2 as a novel enhancer of cerebellar granule cell proliferation. Molecular and cellular neurosciences 57:63-72.

Vogel C, Marcotte EM. 2012. Insights into the regulation of protein abundance from proteomic and transcriptomic analyses. Nature reviews Genetics 13(4):227-232.

Vyas A, Mitra R, Shankaranarayana Rao BS, Chattarji S. 2002. Chronic stress induces contrasting patterns of dendritic remodeling in hippocampal and amygdaloid neurons. The Journal of neuroscience : the official journal of the Society for Neuroscience 22(15):6810-6818.

Wang Z, Jin Y. 2011. Genetic dissection of axon regeneration. Current opinion in neurobiology 21(1):189-196.

Webber CA, Hocking JC, Yong VW, Stange CL, McFarlane S. 2002. Metalloproteases and guidance of retinal axons in the developing visual system. The Journal of neuroscience : the official journal of the Society for Neuroscience 22(18):8091-8100.

Weber AJ, Harman CD. 2008. BDNF preserves the dendritic morphology of alpha and beta ganglion cells in the cat retina after optic nerve injury. Investigative ophthalmology & visual science 49(6):2456-2463.

Wullimann MF, Rupp B, Reichert H. 1996. Neuroanatomy of the Zebrafish Brain. A Topological Atlas: Birkhäuser Basel.

Wyatt C, Ebert A, Reimer MM, Rasband K, Hardy M, Chien CB, Becker T, Becker CG. 2010. Analysis of the astray/robo2 zebrafish mutant reveals that degenerating tracts do not provide strong guidance cues for regenerating optic axons. The Journal of neuroscience : the official journal of the Society for Neuroscience 30(41):13838-13849.

Yazulla S, Studholme KM. 2001. Neurochemical anatomy of the zebrafish retina as determined by immunocytochemistry. Journal of neurocytology 30(7):551-592.

Yong VW, Agrawal SM, Stirling DP. 2007. Targeting MMPs in acute and chronic neurological conditions. Neurotherapeutics : the journal of the American Society for Experimental NeuroTherapeutics 4(4):580-589.

Zhou LX, Wang ZR. 2002. [Changes in number and distribution of retinal ganglion cells after optic nerve crush in zebrafish]. Shi yan sheng wu xue bao 35(2):159-162.

Zou S, Tian C, Ge S, Hu B. 2013. Neurogenesis of retinal ganglion cells is not essential to visual functional recovery after optic nerve injury in adult zebrafish. PloS one 8(2):e57280.

Table and figure legends

Table 1. Antibody table listing specific characteristics of the antibodies used during experiments.

Table 2. Comparison of retinal matrix metalloproteinase (MMP) expression patterns during the four regenerative phases after optic nerve crush (ONC) at RNA (McCurley and Callard, 2010) and protein level. - = downregulation, / = no up- or downregulation; +-+++ = fair to high upregulation.

Figure 1. Mapping of RGC axonal regrowth after ONC in adult zebrafish. A-B Western blotting (WB) for Gap-43 (20-25 kDa) on retinal extracts harvested at different time points after optic nerve crush (ONC) reveals a peak in Gap-43 expression at 4 days post-injury (dpi). For the quantitative analysis, values from ONC samples were plotted relative to sham-operated values, which were put at 100%. Data were collected from minimally 3 retinal samples per time point and are shown as mean ± SEM (* $p < 0.05$). **C** Immunostainings for Gap-43 on retinal sections at various stages post-injury show Gap-43 upregulation in retinal ganglion cell (RGC) somata at 4 dpi and increasing Gap-43 signal in RGC axons from 4-7 dpi. Gap-43 expression re-approaches control levels at 14 dpi. DAPI (blue) was used as nuclear counterstain. Scale bar = 20 μm. **D-E** Microscopic images of biocytin labeled brain sections of uncrushed control fish (UCC) and 7 dpi fish visualizing innervation of the contralateral optic tectum (OT) by RGC axons. Regenerating RGC axons entering the OT at one week post-injury are indicated by arrows. Scale bar = 200 μm (D). Quantification of the

area covered by RGC axons in the OT at 7 dpi, relative to UCC, confirms that axonal regeneration is fully ongoing. Data represent mean ± SEM (n = 5 animals per group, * p < 0.05) (E). ONC, optic nerve crush; dpi, days post-injury; UCC, uncrushed control; NFL, nerve fiber layer; RGCL, retinal ganglion cell layer; IPL, inner plexiform layer; INL, inner nuclear layer; OPL, outer plexiform layer; ONL, outer nuclear layer; PRL, photoreceptor layer.

Figure 2. Retinal broad-spectrum MMP inhibition after ONC reduces OT reinnervation. A Representative images depicting reinnervation of the OT by RGC axons at 7 dpi after PBS, DMSO or GM6001 treatment, reveal a clearly diminished reinnervated OT area after broad-spectrum matrix metalloproteinase (MMP) inhibition (see arrows) as opposed to vehicle control and UCC fish. Scale bar = 200 μm. **B** Quantification of the area covered by RGC axons in the OT of the various treatment conditions, relative to UCC fish. Both, DMSO and PBS treated fish show 60% reinnervation of the OT relative to the completely innervated OT in the UCC condition. A significant reduction in tectal reinnervation was noted in GM6001 treated fish compared to the vehicle controls. Data represent mean ± SEM and 8-15 animals were used per condition over 3 independent experiments (* p < 0.05; ** p < 0.005; *** p < 0.001). UCC, uncrushed control; PBS, phosphate-buffered saline; DMSO, dimethyl sulfoxide.

Figure 3. Lowering general MMP activity after ONC does not influence RGC survival, nor reduce retinal thickness. A-B Representative confocal images of retinal sections immunostained for activated caspase-3 reveals not any apoptotic cell in GM6001 treated eyes at 2 dpi (A) and only a limited number of apoptotic cells in the RGCL at 7 dpi (see arrows) (B). Scale bar = 50 μm. **C** Higher magnifications of an activated caspase-3 immunostaining on retinal sections of PBS, DMSO and GM6001 treated fish indicate a similar amount of apoptotic RGCs at 7 dpi in the three conditions, while apoptosis is absent in UCC fish. Moreover, no obvious disruption of retinal structure, nor retinal thinning can be observed in GM6001-injected fish. Scale bar = 20 μm. DAPI (blue) was used as nuclear counterstain. **D** Quantitative analysis of the ratio of activated Caspase-3$^+$ cells/DAPI$^+$ cells in the RGCL reveals no difference between PBS, DMSO and GM6001 treated fish at 7 dpi. Data represent 5 fish per group and are shown as mean ± SEM. **E** Likewise, the number of DAPI$^+$ cells per 100 μm was found similar in all conditions, both at 2 and 7 dpi, confirming that no significant cell loss is induced after ONC/treatment. Data represent 5 fish per group and are shown as mean ± SEM. **F** No significant differences in retinal thickness of uninjected, PBS, DMSO and GM6001 treated fish at 7 dpi were observed after quantitative analysis. Per fish, 6 retinal sections were analyzed, using 5 fish per condition. Data are shown as mean ± SEM. Dpi, days post-injury; PBS, phosphate-buffered saline; DMSO, dimethyl sulfoxide; NFL, nerve fiber layer; RGCL, retinal ganglion cell layer; IPL, inner plexiform layer; INL, inner nuclear layer; OPL, outer plexiform layer; ONL, outer nuclear layer; PRL, photoreceptor layer.

Figure 4. Retinal spatiotemporal expression pattern of Mmp-13a protein after ONC in adult zebrafish. A-B Representative picture and bar graph revealing Western blotting analysis data for Mmp-13a on retinal extracts after ONC, showing significantly increased active Mmp-13a (45 kDa) levels at 7 dpi, represented as a relative percentage to sham-operated values. No differences in pro Mmp-13a (80 kDa) were observed. Data were collected from minimally 3 retinal samples per time point and are shown as mean ± SEM (** $p <$ 0.005). **C** Immunohistochemical staining for Mmp-13a on retinal sections of sham-operated and crushed fish, ascribing an elevated Mmp-13a signal in the RGCL at 7 dpi, during axonal regrowth. DAPI (blue) was used as nuclear counterstain. Scale bar = 20 μm. **D** High magnification photographs of the RGCs after H&E, immunofluorescent or DAB staining for Mmp-13a, altogether indicating expression of Mmp-13a in RGC somata and primary dendrites after ONC. DAPI (blue) or hematoxylin was used as nuclear counterstain. ONC, optic nerve crush; dpi, days post-injury; NFL, nerve fiber layer; RGCL, retinal ganglion cell layer; IPL, inner plexiform layer; INL, inner nuclear layer; OPL, outer plexiform layer; ONL, outer nuclear layer; PRL, photoreceptor layer.

Figure 5. Retinal spatiotemporal expression pattern of Mmp-2 protein after ONC in adult zebrafish. A Representative picture showing the presence of active Mmp-2 in adult zebrafish retinal extracts, as confirmed by labeling of both pro (72 kDa) and active (64 kDa) Mmp-2 in zebrafish embryo lysates (left). **A-B** Western blotting for Mmp-2 on retinal extracts at different time points post-injury indicates a peak in active Mmp-2 expression at 10 dpi during retinotectal regeneration, as compared to sham-operated controls (put at 100%). Data represent minimally 3 retinal samples per time point and are shown as mean ± SEM (* $p <$ 0.05). **C** Double immunostaining for α-tubulin and Mmp-2 on retinal sections indicates expression of Mmp-2 in/on RGC axons. Left scale bar = 20 μm. Scale bars on highly magnified images (right) are 5 μm. **D** Immunostainings for Mmp-2 on retinal sections at 4 dpi disclose a decreased expression of Mmp-2 in RGC axons compared to controls, but an increased presence in RGC somata. During axonal regrowth, Mmp-2 expression becomes upregulated in RGC somata and axons, whereafter its expression again confines to RGC axons. Scale bars are 20 μm. For all immunostainings, DAPI (blue) was used as a nuclear counterstain. ONC, optic nerve crush; dpi, days post-injury; NFL, nerve fiber layer; RGCL, retinal ganglion cell layer; IPL, inner plexiform layer; INL, inner nuclear layer; OPL, outer plexiform layer; ONL, outer nuclear layer; PRL, photoreceptor layer.

Figure 6. Retinal spatiotemporal expression pattern of Mmp-14 protein after ONC in adult zebrafish. A-B Representative picture and bar graph revealing Western blotting analysis data for Mmp-14 on retinal extracts after ONC, respectively showing significantly increased mature Mmp-14 (55-60 kDa) levels at 6 hpi and decreased levels at 10 dpi. Values from ONC samples were plotted relative to sham-operated values, which were put at 100%. Data represent minimally 3 retinal samples per time point and are shown as mean ± SEM (* $p <$ 0.05). **C** Immunostainings for Mmp-14 on retinal sections harvested at varying days after

ONC equally show an upregulation of Mmp-14 in the nerve fiber layer (NFL) and inner plexiform layer (IPL) at 6 hours post-injury (hpi) and a decrease herein during axonal regrowth. Scale bars are 20 μm. **D** Double labeling of retinal sections for MAP2 and Mmp-14, reveals Mmp-14 expression in IPL neurites at 6 hpi. Left scale bar = 20 μm. Scale bars on highly magnified images (right) are 5 μm. **E** Double staining for α-tubulin and Mmp-14, indicates expression of Mmp-14 in/on RGC axons in retinal sections of control sham-operated fish. Left scale bar = 20 μm. Scale bars on highly magnified images (right) are 5 μm. For all immunostainings, DAPI (blue) was used as a nuclear counterstain. ONC, optic nerve crush; hpi, hours post-injury; dpi, days post-injury; NFL, nerve fiber layer; RGCL, retinal ganglion cell layer; IPL, inner plexiform layer; INL, inner nuclear layer; OPL, outer plexiform layer; ONL, outer nuclear layer; PRL, photoreceptor layer.
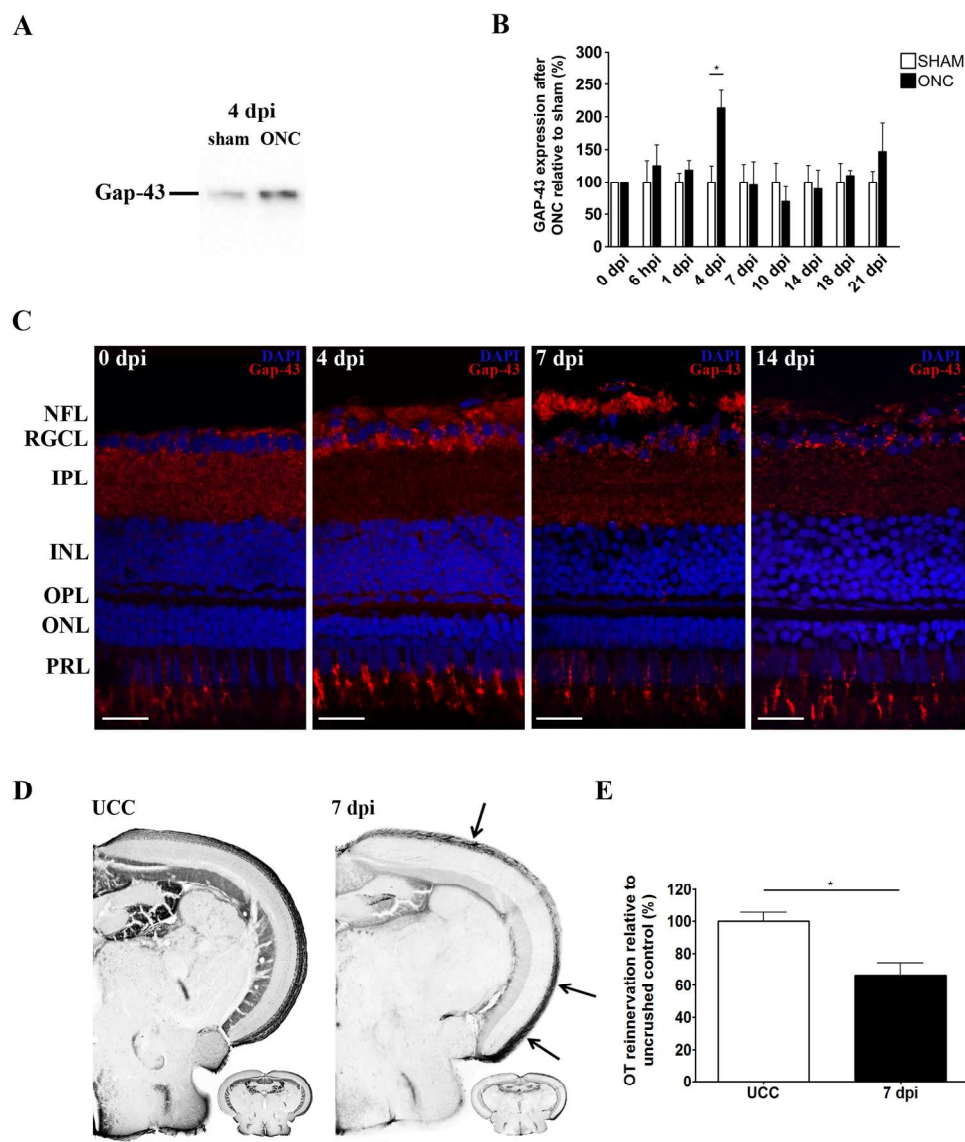
Figure 7. Retinal spatiotemporal expression pattern of Mmp-9 protein after ONC in adult zebrafish. A Representative picture showing presence of active Mmp-9 in zebrafish retinal extracts, as confirmed by labeling of both pro (92 kDa) and active (76 kDa) Mmp-9 in zebrafish embryo lysates (left). **A-B** Western blotting for Mmp-9 on retinal extracts at different time points post-injury indicates a peak in active Mmp-9 expression at 14 dpi compared to sham-operated controls. Data represent minimally 3 retinal samples per time point and are shown as mean ± SEM (* p < 0.05). **C** Immunostainings for Mmp-9 on retinal sections, show an increased Mmp-9 signal in 3 prominent IPL strata at 14 dpi. Scale bars are 20 μm. **D** Double staining with SV2 confirms expression of Mmp-9 in a subset of IPL synapses. Left scale bar = 20 μm. Scale bars on highly magnified images (right) are 5 μm. For all immunostainings, DAPI (blue) was used as a nuclear counterstain. ONC, optic nerve crush; dpi, days post-injury; NFL, nerve fiber layer; RGCL, retinal ganglion cell layer; IPL, inner plexiform layer; INL, inner nuclear layer; OPL, outer plexiform layer; ONL, outer nuclear layer; PRL, photoreceptor layer.

Figure 1. Mapping of RGC axonal regrowth after ONC in adult zebrafish. A-B Western blotting (WB) for Gap-43 (20-25 kDa) on retinal extracts harvested at different time points after optic nerve crush (ONC) reveals a peak in Gap-43 expression at 4 days post-injury (dpi). For the quantitative analysis, values from ONC samples were plotted relative to sham-operated values, which were put at 100%. Data were collected from minimally 3 retinal samples per time point and are shown as mean ± SEM (* p < 0.05). C Immunostainings for Gap-43 on retinal sections at various stages post-injury show Gap-43 upregulation in retinal ganglion cell (RGC) somata at 4 dpi and increasing Gap-43 signal in RGC axons from 4-7 dpi. Gap-43 expression re-approaches control levels at 14 dpi. DAPI (blue) was used as nuclear counterstain. Scale bar = 20 μm. D-E Microscopic images of biocytin labeled brain sections of uncrushed control fish (UCC) and 7 dpi fish visualizing innervation of the contralateral optic tectum (OT) by RGC axons. Regenerating RGC axons entering the OT at one week post-injury are indicated by arrows. Scale bar = 200 μm (D). Quantification of the area covered by RGC axons in the OT at 7 dpi, relative to UCC, confirms that axonal regeneration is fully ongoing. Data represent mean ± SEM (n = 5 animals per group, * p < 0.05) (E). ONC, optic nerve crush;

dpi, days post-injury; UCC, uncrushed control; NFL, nerve fiber layer; RGCL, retinal ganglion cell layer; IPL, inner plexiform layer; INL, inner nuclear layer; OPL, outer plexiform layer; ONL, outer nuclear layer; PRL, photoreceptor layer.
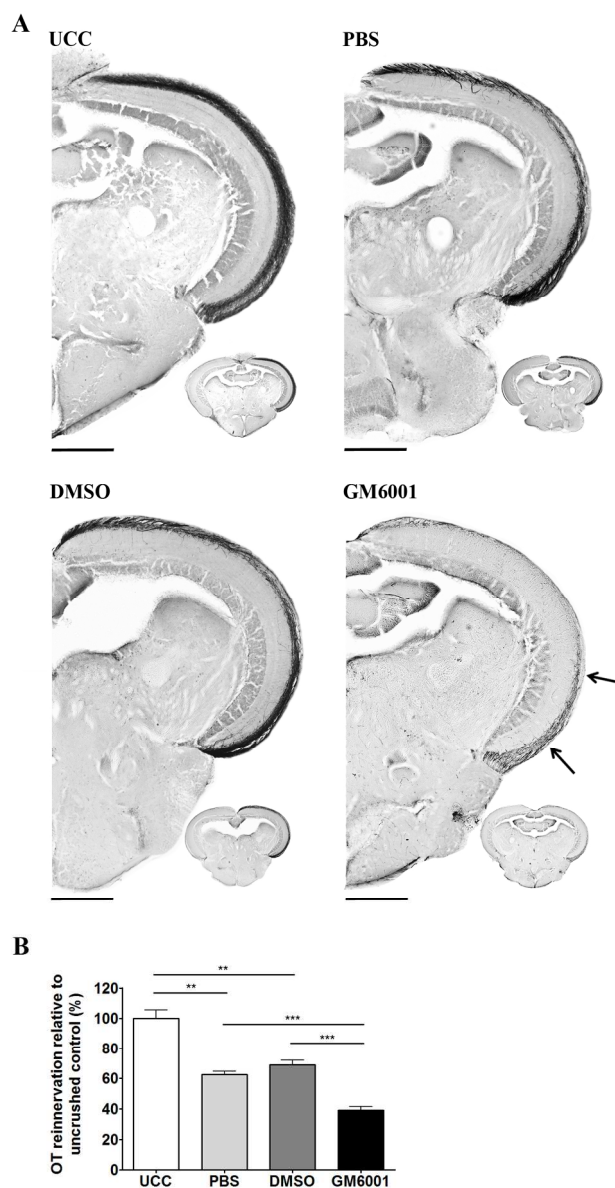171x207mm (300 x 300 DPI)

Figure 2. Retinal broad-spectrum MMP inhibition after ONC reduces OT reinnervation. A Representative images depicting reinnervation of the OT by RGC axons at 7 dpi after PBS, DMSO or GM6001 treatment, reveal a clearly diminished reinnervated OT area after broad-spectrum matrix metalloproteinase (MMP) inhibition (see arrows) as opposed to vehicle control and UCC fish. Scale bar = 200 µm. B Quantification of the area covered by RGC axons in the OT of the various treatment conditions, relative to UCC fish. Both, DMSO and PBS treated fish show 60% reinnervation of the OT relative to the completely innervated OT in the UCC condition. A significant reduction in tectal reinnervation was noted in GM6001 treated fish compared to the vehicle controls. Data represent mean ± SEM and 8-15 animals were used per condition over 3 independent experiments (* $p < 0.05$; ** $p < 0.005$; *** $p < 0.001$). UCC, uncrushed control; PBS, phosphate-buffered saline; DMSO, dimethyl sulfoxide.
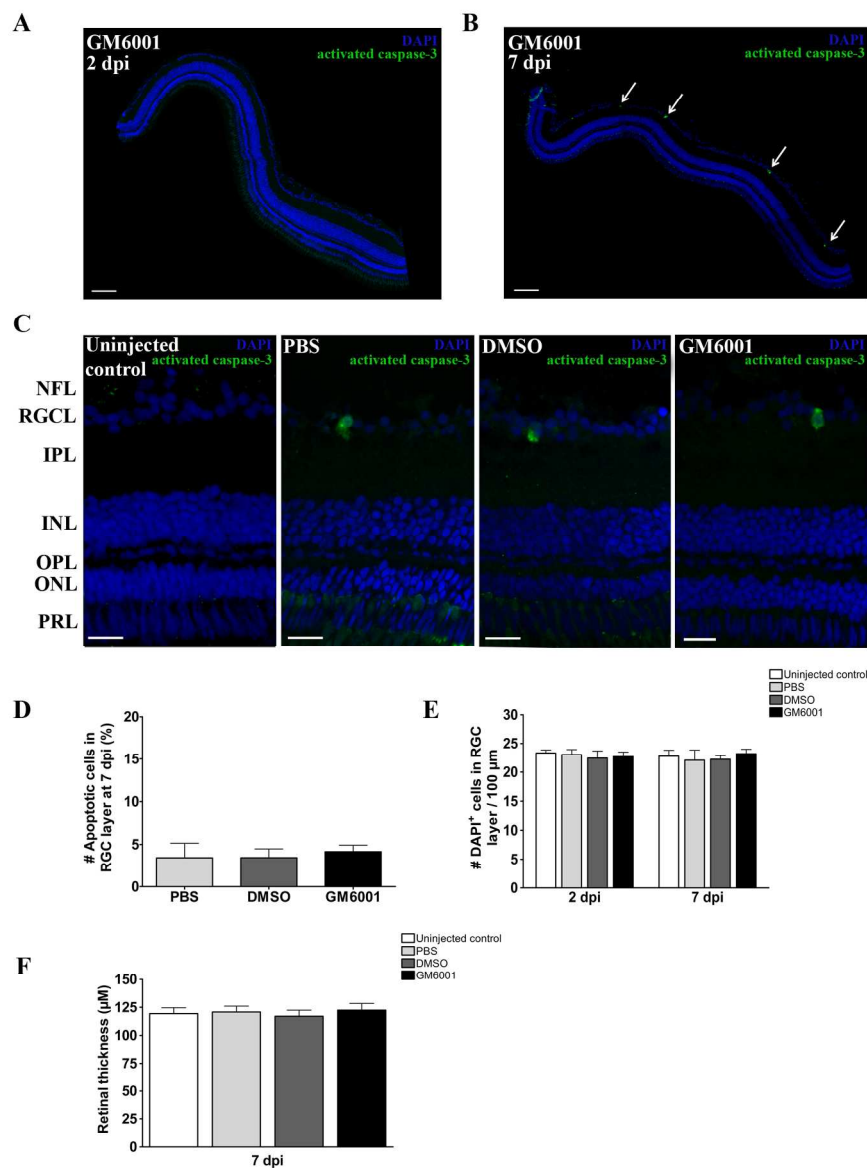130x230mm (300 x 300 DPI)

Figure 3. Lowering general MMP activity after ONC does not influence RGC survival, nor reduce retinal thickness. A-B Representative confocal images of retinal sections immunostained for activated caspase-3 reveals not any apoptotic cell in GM6001 treated eyes at 2 dpi (A) and only a limited number of apoptotic cells in the RGCL at 7 dpi (see arrows) (B). Scale bar = 50 μm. C Higher magnifications of an activated caspase-3 immunostaining on retinal sections of PBS, DMSO and GM6001 treated fish indicate a similar amount of apoptotic RGCs at 7 dpi in the three conditions, while apoptosis is absent in UCC fish. Moreover, no obvious disruption of retinal structure, nor retinal thinning can be observed in GM6001-injected fish. Scale bar = 20 μm. DAPI (blue) was used as nuclear counterstain. D Quantitative analysis of the ratio of activated Caspase-3+ cells/DAPI+ cells in the RGCL reveals no difference between PBS, DMSO and GM6001 treated fish at 7 dpi. Data represent 5 fish per group and are shown as mean ± SEM. E Likewise, the number of DAPI+ cells per 100 μm was found similar in all conditions, both at 2 and 7 dpi, confirming that no significant cell loss is induced after ONC/treatment. Data represent 5 fish per group and are shown as mean ± SEM. F No significant differences in retinal thickness of uninjected, PBS, DMSO and GM6001 treated

fish at 7 dpi were observed after quantitative analysis. Per fish, 6 retinal sections were analyzed, using 5 fish per condition. Data are shown as mean ± SEM. Dpi, days post-injury; PBS, phosphate-buffered saline; DMSO, dimethyl sulfoxide; NFL, nerve fiber layer; RGCL, retinal ganglion cell layer; IPL, inner plexiform layer; INL, inner nuclear layer; OPL, outer plexiform layer; ONL, outer nuclear layer; PRL, photoreceptor layer.
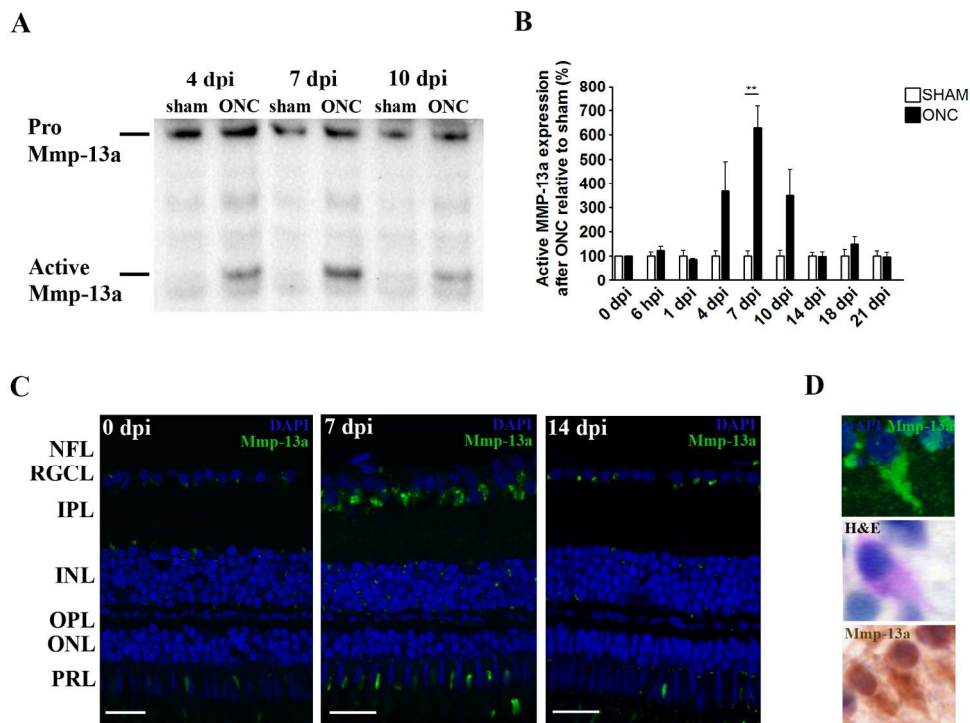
171x230mm (300 x 300 DPI)

Figure 4. Retinal spatiotemporal expression pattern of Mmp-13a protein after ONC in adult zebrafish. A-B Representative picture and bar graph revealing Western blotting analysis data for Mmp-13a on retinal extracts after ONC, showing significantly increased active Mmp-13a (45 kDa) levels at 7 dpi, represented as a relative percentage to sham-operated values. No differences in pro Mmp-13a (80 kDa) were observed. Data were collected from minimally 3 retinal samples per time point and are shown as mean ± SEM (** $p < 0.005$). C Immunohistochemical staining for Mmp-13a on retinal sections of sham-operated and crushed fish, ascribing an elevated Mmp-13a signal in the RGCL at 7 dpi, during axonal regrowth. DAPI (blue) was used as nuclear counterstain. Scale bar = 20 µm. D High magnification photographs of the RGCs after H&E, immunofluorescent or DAB staining for Mmp-13a, altogether indicating expression of Mmp-13a in RGC somata and primary dendrites after ONC. DAPI (blue) or hematoxylin was used as nuclear counterstain. ONC, optic nerve crush; dpi, days post-injury; NFL, nerve fiber layer; RGCL, retinal ganglion cell layer; IPL, inner plexiform layer; INL, inner nuclear layer; OPL, outer plexiform layer; ONL, outer nuclear layer; PRL, photoreceptor layer.
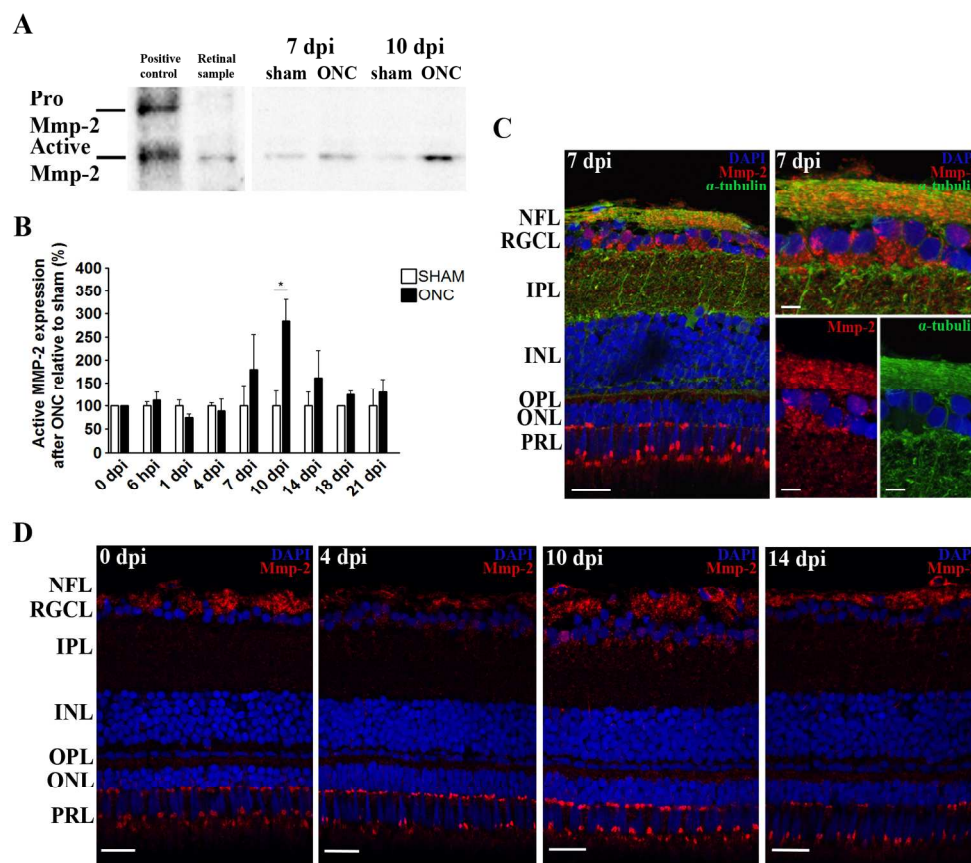171x129mm (300 x 300 DPI)

Figure 5. Retinal spatiotemporal expression pattern of Mmp-2 protein after ONC in adult zebrafish. A Representative picture showing the presence of active Mmp-2 in adult zebrafish retinal extracts, as confirmed by labeling of both pro (72 kDa) and active (64 kDa) Mmp-2 in zebrafish embryo lysates (left). A-B Western blotting for Mmp-2 on retinal extracts at different time points post-injury indicates a peak in active Mmp-2 expression at 10 dpi during retinotectal regeneration, as compared to sham-operated controls (put at 100%). Data represent minimally 3 retinal samples per time point and are shown as mean ± SEM (* p < 0.05). C Double immunostaining for α-tubulin and Mmp-2 on retinal sections indicates expression of Mmp-2 in/on RGC axons. Left scale bar = 20 μm. Scale bars on highly magnified images (right) are 5 μm. D Immunostainings for Mmp-2 on retinal sections at 4 dpi disclose a decreased expression of Mmp-2 in RGC axons compared to controls, but an increased presence in RGC somata. During axonal regrowth, Mmp-2 expression becomes upregulated in RGC somata and axons, whereafter its expression again confines to RGC axons. Scale bars are 20 μm. For all immunostainings, DAPI (blue) was used as a nuclear counterstain. ONC, optic nerve crush; dpi, days post-injury; NFL, nerve fiber layer; RGCL, retinal ganglion cell layer; IPL, inner plexiform layer; INL, inner nuclear layer; OPL, outer plexiform layer; ONL, outer nuclear layer; PRL, photoreceptor layer.
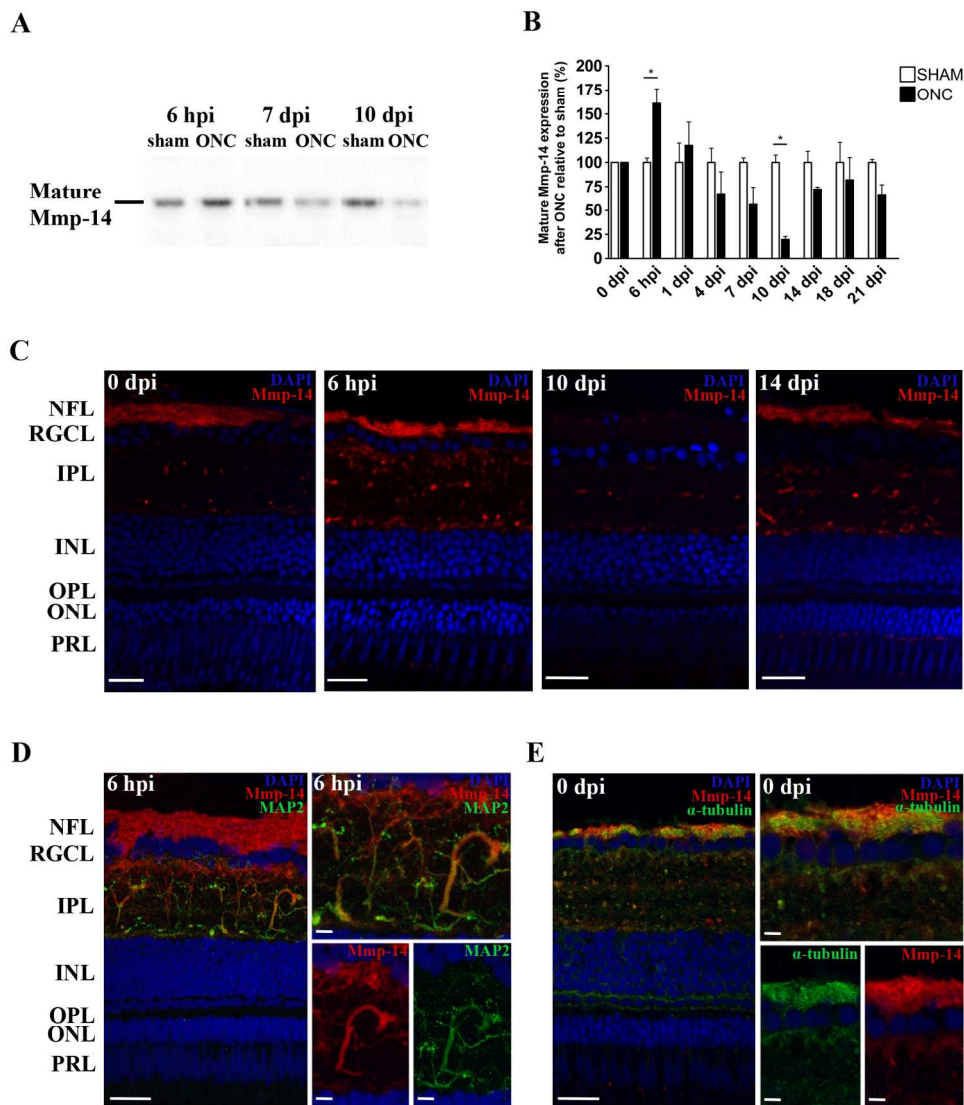171x153mm (300 x 300 DPI)

Figure 6. Retinal spatiotemporal expression pattern of Mmp-14 protein after ONC in adult zebrafish. A-B Representative picture and bar graph revealing Western blotting analysis data for Mmp-14 on retinal extracts after ONC, respectively showing significantly increased mature Mmp-14 (55-60 kDa) levels at 6 hpi and decreased levels at 10 dpi. Values from ONC samples were plotted relative to sham-operated values, which were put at 100%. Data represent minimally 3 retinal samples per time point and are shown as mean ± SEM (* p < 0.05). C Immunostainings for Mmp-14 on retinal sections harvested at varying days after ONC equally show an upregulation of Mmp-14 in the nerve fiber layer (NFL) and inner plexiform layer (IPL) at 6 hours post-injury (hpi) and a decrease herein during axonal regrowth. Scale bars are 20 µm. D Double labeling of retinal sections for MAP2 and Mmp-14, reveals Mmp-14 expression in IPL neurites at 6 hpi. Left scale bar = 20 µm. Scale bars on highly magnified images (right) are 5 µm. E Double staining for α-tubulin and Mmp-14, indicates expression of Mmp-14 in/on RGC axons in retinal sections of control sham-operated fish. Left scale bar = 20 µm. Scale bars on highly magnified images (right) are 5 µm. For all immunostainings, DAPI (blue) was used as a nuclear counterstain. ONC, optic nerve crush; hpi, hours post-injury; dpi, days post-injury; NFL, nerve fiber layer; RGCL, retinal ganglion cell layer; IPL, inner plexiform layer; INL, inner nuclear layer; OPL, outer plexiform layer; ONL, outer nuclear layer; PRL, photoreceptor
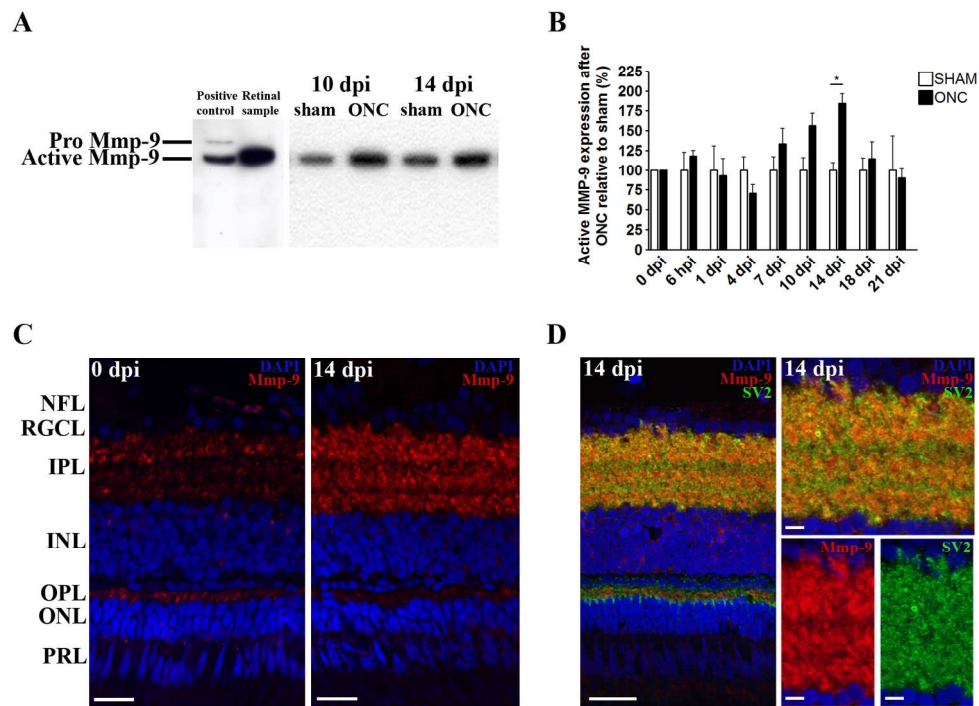
layer.
171x196mm (300 x 300 DPI)

Figure 7. Retinal spatiotemporal expression pattern of Mmp-9 protein after ONC in adult zebrafish. A Representative picture showing presence of active Mmp-9 in zebrafish retinal extracts, as confirmed by labeling of both pro (92 kDa) and active (76 kDa) Mmp-9 in zebrafish embryo lysates (left). A-B Western blotting for Mmp-9 on retinal extracts at different time points post-injury indicates a peak in active Mmp-9 expression at 14 dpi compared to sham-operated controls. Data represent minimally 3 retinal samples per time point and are shown as mean ± SEM (* $p < 0.05$). C Immunostainings for Mmp-9 on retinal sections, show an increased Mmp-9 signal in 3 prominent IPL strata at 14 dpi. Scale bars are 20 µm. D Double staining with SV2 confirms expression of Mmp-9 in a subset of IPL synapses. Left scale bar = 20 µm. Scale bars on highly magnified images (right) are 5 µm. For all immunostainings, DAPI (blue) was used as a nuclear counterstain. ONC, optic nerve crush; dpi, days post-injury; NFL, nerve fiber layer; RGCL, retinal ganglion cell layer; IPL, inner plexiform layer; INL, inner nuclear layer; OPL, outer plexiform layer; ONL, outer nuclear layer; PRL, photoreceptor layer.
171x131mm (300 x 300 DPI)

Table 1. Antibody table listing specific characteristics of the antibodies used during experiments.

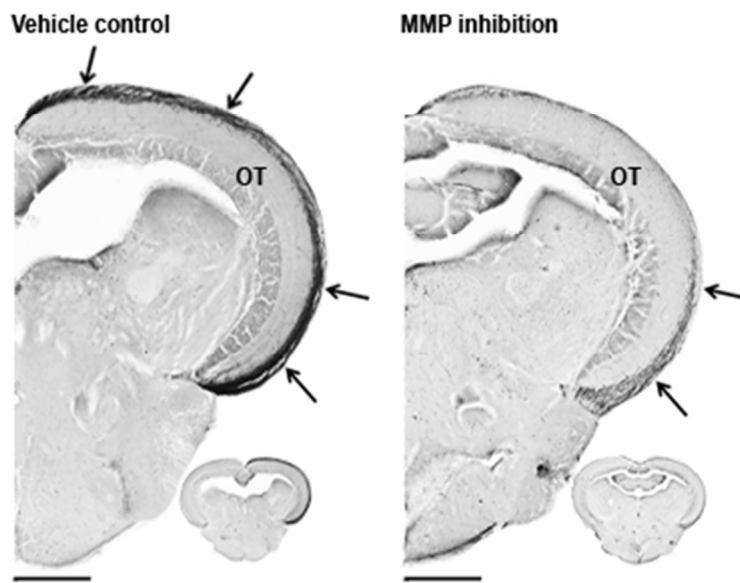| Antibody	Immunogen Structure	Manufacturer, Catalog Number, RRID, Species, Monoclonal or Polyclonal	Concentration
Mmp-2	Peptide near C-terminus of human MMP-2 (aa 600-650)	Santa Cruz Biotechnology, sc-8835-R, AB_1565437, rabbit, polyclonal	IHC: 1/200 WB: 1/100
Mmp-14	Synthetic peptide to C-terminus of human MMP-14 (aa 471-520)	Abcam, ab53712, AB_881233, rabbit, polyclonal	IHC: 1/200 WB: 1/1000
Mmp-9	Synthetic peptide to hinge region of zebrafish Mmp-9 (aa 440-480)	Anaspec, AS-55345, AB_2144746, rabbit, polyclonal	IHC: 1/200 WB: 1/1000
Mmp-13a	Synthetic peptide to hinge region of zebrafish Mmp-13 (aa 185-285)	Anaspec, AS-55114, AB_1657437, rabbit, polyclonal	IHC: 1/200 WB: 1/250
Gap-43	Full-length GAP-43 of rat origin	Santa Cruz Biotechnology, sc-33705, AB_627659, mouse, monoclonal	IHC: 1/300 WB: 1/1000
Alpha-tubulin	Purified chick brain tubulin	Sigma-Aldrich, T9026, AB_477593, mouse, monoclonal	IHC: 1/200
MAP2 (2a+2b)	Bovine MAP2	Sigma-Aldrich, M1406, AB_477171, mouse, monoclonal	IHC: 1/500
Activated Caspase-3	Synthetic peptide to N-terminus adjacent to cleavage site human caspase-3	Biovision, 3015-100, AB_2069697, rabbit, polyclonal	IHC: 1/75
SV2	Highly purified vesicles from the electric organ of *Discopyge ommata*	Developmental Studies Hybridoma Bank, SV2, AB_528480, mouse, monoclonal	IHC: 1/1000

Table 2. Comparison of retinal matrix metalloproteinase (MMP) expression patterns during the four regenerative phases after optic nerve crush (ONC) at RNA (McCurley and Callard, 2010) and protein level.

MMP	RNA/Protein level	Injury response	Axonal regrowth	Axonal extension	Synaptic refinement
MMP-13a	RNA	+++ (top ten)	+	/	/
	Protein	/	+++	+	/
MMP-9	RNA	++ (top ten)	+++	+	/
	Protein	/	/	++	/
MMP-2	RNA	/	+	/	/
	Protein	/	+	++	/
MMP-14	RNA	/	++	+	/
	Protein	+	-	-/	/

(Legend: - = downregulation; / = no up- or downregulation; +-+++ = fair to high upregulation.)

The authors show that *in vivo* retinal broad-spectrum matrix metalloproteinase (MMP) inhibition strongly reduced optic tectum (OT) reinnervation by regenerating retinal ganglion cell axons at 7 days after optic nerve crush in adult zebrafish. MMP signalling pathways thus appear critical for axonal regrowth, providing conceptual insights for novel regenerative therapies.

141x105mm (72 x 72 DPI)